AN ABSTRACT OF THE THESIS OF

SCOTT LYMAN BOLEY   for the   MASTER OF SCIENCE
_____   _____
(Name)   (Degree)

in   OCEAN ENGINEERING   presented on   MAY 4, 1973
       _____   _____
       (Major)   (Date)

Title: DISCHARGE COEFFICIENT OF AN ESTUARINE ENTRANCE

Abstract approved: Redacted for Privacy
                              Dr. Larry S. Slotta

An estuarine entrance was examined as a hydraulic nozzle or orifice. Field studies were conducted to determine the discharge coefficient of a natural inlet for both flood and ebb tidal flows. The discharge coefficient was found to significantly vary throughout the tidal cycle. A strong relationship was found between the discharge coefficient and velocity through the inlet.

Measured energy losses across the inlet were compared with losses predicted from studies of the inlet bathymetry. For the ebb tide, measured energy losses across the inlet compared unfavorably with those predicted. This indicates that factors other than inlet shape can exert a dominating influence upon the tidal discharge rate through the inlet. Resistance to flow occurring upstream of the inlet could be such a factor. However, favorable comparison of predicted and neasured losses across the inlet for incoming flows indicates that the inlet shape and hydraulic characteristics are critical factors affecting

the tidal response of the estuary during the flooding tide. Analysis of an esturay based upon a detailed knowledge of the inlet bathymetry can provide valuable insight into the hydraulic behavior of the estuary, and may provide a means of determining what effect inlet modifications will have on the tidal response of the estuary.

Discharge Coefficient of an Estuarine Entrance

by

Scott Lyman Boley

A THESIS

submitted to

Oregon State University

in partial fulfillment of
the requirements for the
degree of

Master of Ocean Engineering

June 1974

APPROVED:

Redacted for Privacy

Associate Professor of Civil Engineering and
Director of Ocean Engineering
in charge of major

Redacted for Privacy

Chairman of Civil Engineering

Redacted for Privacy

Dean of Graduate School

Date thesis is presented   May 4, 1973

Typed by Opal Grossnicklaus for Scott Lyman Boley

ACKNOWLEDGEMENT

TABLE OF CONTENTS

LIST OF FIGURES

LIST OF APPENDIX FIGURES

LIST OF TABLES

LIST OF APPENDIX TABLES

LIST OF SYMBOLS

γ - specific gravity

λ - friction factor

θ - specific tidal time in radians

A, A_c - cross sectional area

A_s - surface area of bay

a_o - ocean tidal amplitude

C - discharge coefficient

g - gravitational acceleration

H - ratio of water surface height to tidal range

h - height of the water surface above the reference level

K - coefficient of repletion

L - length of inlet

m - entrance-exit loss coefficient

n - Manning's friction factor

P - pressure

Q - flow rate

R - hydraulic radius

S - water surface slope

T - tidal period

V - velocity

DISCHARGE COEFFICIENT OF AN ESTUARINE ENTRANCE

I. INTRODUCTION

It is the intent of this study to examine the possible behavior of an esturay entrance as a hydraulic nozzle or orifice. By considering flow through the entrance to be similar to flow through a nozzle, the basis for simple useful relationships between discharge and head losses may be developed to further the understanding of tidal hydraulics and aid estuarine and land use planners in determining proper utilization of an estuary.

An inlet, defined by O'Brien (1971) as the connecting channel between the ocean and an estuary or lagoon, is affected by many factors. Wave induced longshore transport of sand is continually filling the inlet, with the rate of sand inflow dependent upon the amplitude, frequency, and direction of the incoming waves. Tidal flow into and out of the estuary however will tend to erode or cut away this sand, until ideally an equilibrium is reached between the filling and erosional processes. This equilibrium configuration of the inlet is dependent upon the tidal prism of the estuary or lagoon. The tidal prism of an estuary is the volume of water entering between mean lower low water and mean higher high water, and this volume of water will determine the erosional capability of the inlet.

Jetties are often constructed to improve an inlet for navigation.

The spacing of these jetties is determined by the tidal prism of the estuary and the desired depth of the entrance channel. The length of the jetties is determined by the width of the littoral drift zone and the need to protect craft using the inlet from wave activity. Construction of jetties usually increases the mean depth of the inlet, decreases the width, and increases the length of the inlet.

What effect do these modifications of the inlet have on the tidal response of the lagoon or estuary? To answer this question physical and numerical models are developed and calibrated, usually at great expense. However if the inlet could be treated as a hydraulic nozzle, this might prove to be useful for understanding the effects of inlet changes at a significant reduction in cost.

It was beyond the scope of this study to develop predictive relationships from which to evaluate the effect upon an estuary of possible inlet modifications. The intent of this study is to determine whether it is valid to treat an estuarine inlet as a hydraulic nozzle. It is hoped this study might advance our understanding of the hydraulic factors affecting our estuaries.

II. CONCEPTS AND THEORETICAL CONSIDERATIONS

Consider an ocean-bay system as depicted below.
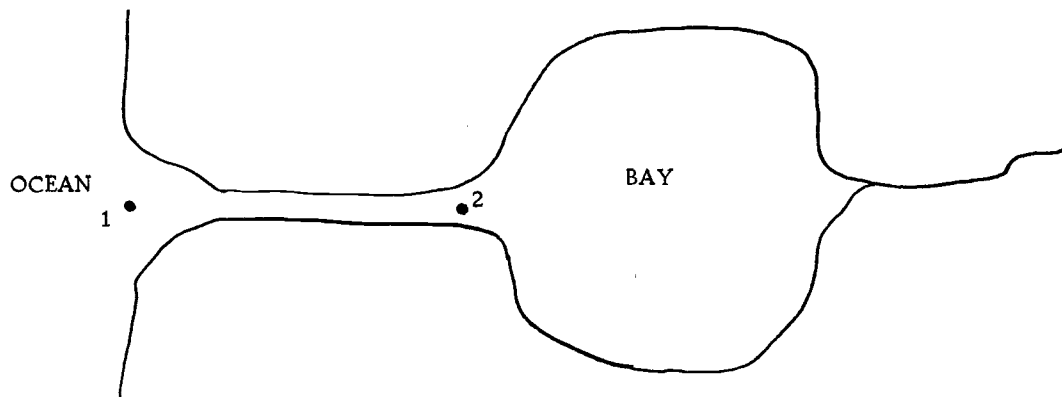
Let h_1 be the elevation of the ocean above some reference level, and h_2 the elevation of the bay.
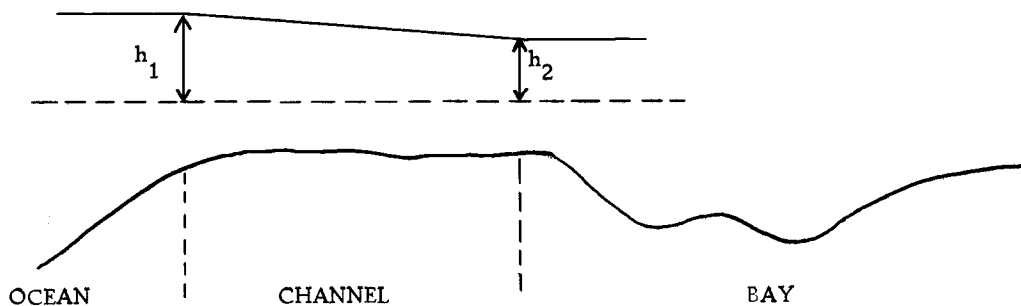
Conceptual Bay-Ocean System

Writing Bernoulli's equation for points 1 and 2

$$\frac{P_1}{\gamma} + \frac{V_1^2}{2g} + h_1 = \frac{P_2}{\gamma} + \frac{V_2^2}{2g} + h_2 + \text{head loss,} \qquad (1)$$

we see that since $P_1 = P_2 =$ atmospheric, and from the continuity

equation $V_1 A_1 = V_2 A_2$, where A_1 and A_2 are the cross sectional areas

at points 1 and 2 respectively, Bernoulli's equation reduces to

$$h_1 - h_2 = \frac{V_2^2}{2g} \left(1 - \frac{A_2}{A_1}^2\right) + \text{head loss.} \quad \text{[ft]} \tag{2}$$

If we assume $A_1 \gg A_2$, this reduces to

$$h_1 - h_2 = \frac{V_2^2}{2g} + \text{head loss.} \quad \text{[ft]} \tag{3}$$

The head loss across the inlet can be broken into two parts, one part

being the energy necessary to overcome entrance and exit losses,

and the other part the energy dissipated due to friction in the inlet.

Using the Darcy-Weisbach formula for friction losses, one gets

$$h_1 - h_2 = \left(m + \frac{\lambda L}{R}\right) \frac{V^2}{2g} \tag{4}$$

where m is a measure of entrance and exit losses,

   R is the hydraulic radius of the entrance channel,

   λ is the friction factor, and

   L is the length of the inlet.

Solving for V^2 yields

$$V^2 = 2g \left(\frac{1}{m} + \frac{R}{\lambda L}\right)(h_1 - h_2). \tag{5}$$

Taking the square root, rearranging and multiplying by the cross sectional area of the entrance channel yields the discharge relationship

$$VA_c = A_c \left[\left(\frac{R}{\lambda L} + \frac{1}{m} \right) 2g (h_1 - h_2) \right]^{\frac{1}{2}} \tag{6}$$

where A_c is cross sectional area of entrance channel.

Letting
$$C = \left[\frac{R}{\lambda L} + \frac{1}{m} \right]^{\frac{1}{2}}$$

one gets
$$Q = CA_c \sqrt{2g(h_1 - h_2)}. \quad [\text{ft}^3/\text{sec}] \tag{7}$$

C is the inlet discharge coefficient as suggested by O'Brien (1971), and is a combination of frictional effects and channel shape. To determine C one only needs to know the tidal heights of the basin and ocean, the flow rate, and the entrance cross sectional area. If indeed C varies in some predictable manner with channel shape and roughness, then by knowing the value of C for some particular entrance configuration and the determining cross sectional area, one would be able to predict with confidence the flow rates into an estuary and velocities through the entrance.

In model studies of Galveston Bay (Sager, 1973) the U. S. Army Corps of Engineers used the discharge coefficient to compare the efficiency of different inlet configurations in passing flows resulting from a hurricane surge. A higher discharge coefficient would indicate

a more efficient inlet configuration. The discharge coefficient was found to vary from 0.3 to 0.6, with a mean value of 0.47 for hurricane surge conditions and 0.35 for normal tidal conditions.

Keulegan (1967) presented an analysis concerning tidal discharges through an inlet whereby he obtained what he termed a coefficient of filling or repletion for an estuary. Keulegan's coefficient of repletion was derived assuming an entrance channel with vertical walls, uniform cross section, and a depth much greater than the tidal range. The expression for this coefficient is

$$K = \frac{T}{2\pi a_o} \frac{A_c}{A_s} \sqrt{\frac{2gRa_o}{\lambda L + mR}} \tag{8}$$

where   T = tidal period,

   a_o = ocean tidal amplitude,

   A_s = surface area of the bay,

and the other terms are as previously defined. It can be shown that the discharge coefficient C and the repletion coefficient K are related by

$$K = C \frac{T}{2\pi a_o} \frac{A_c}{A_s} \sqrt{2g\, a_o} \quad [\text{dimensionless}] \tag{9}$$

It is apparent that while K is a measure of the filling of the whole estuary, summarizing the effects of channel and basin dimensions, tidal range, period, and entrance roughness, the discharge coefficient C is concerned only with the entrance region, and that determining

the value of C will aid in determining the value of Keulegan's repletion coefficient, K.

Using the repletion coefficient, the change in water level height in the estuary is given by

$$\frac{dH_2}{d\theta} = K \sqrt{H_1 - H_2} \qquad [ft] \qquad (10)$$

where θ = specific tidal time in radians,

    H_1 = ratio of water height outside to ocean tidal amplitude,

and H_2 = ratio of water height inside to ocean tidal amplitude.

This assumes no stream inflow to the basin.

III. STUDY SITE

General Description

Alsea Bay is an estuary located on the mid-Oregon coast,
latitude $44^\circ 26'$ North and longitude $124^\circ 05'$ West, about 130 miles
south of the Columbia River mouth, as shown in Figure 1. The
estuary has a drainage basin of 474 square miles composed princi-
pally of the Alsea River basin. This contributes an average fresh
water inflow to the estuary of 2070 cfs, with a maximum observed
flow of 42,000 cfs during periods of high winter runoff, and a mini-
mum flow of less than 100 cfs during late summer and early fall. The
estuary surface area is reported by Marriage (1958) to be 2,227
acres, with tidelands composing 46 percent of this area. The tides
affecting Alsea Bay are of a semidiurnal nature, with a mean tidal
range of 5.8 feet, a diurnal range of 7.7 feet, and a tidal prism
(MHHW-MLLW) of 5×10^8 cubic feet, as reported by Goodwin (1970).

The only incorporated town in the area is Waldport, 1970 popu-
lation 700, located on the south side of the bay. Commercial use of
the estuary is quite minor, limited principally to the taking of crabs,
clams, and sand shrimp. Recreational use of the estuary is quite
extensive, including fishing, boating, crabbing, clamming and agate
hunting. The Aleas River and estuary support large runs of steelhead
and salmon, with an annual sport harvest of over 14,000 fish.
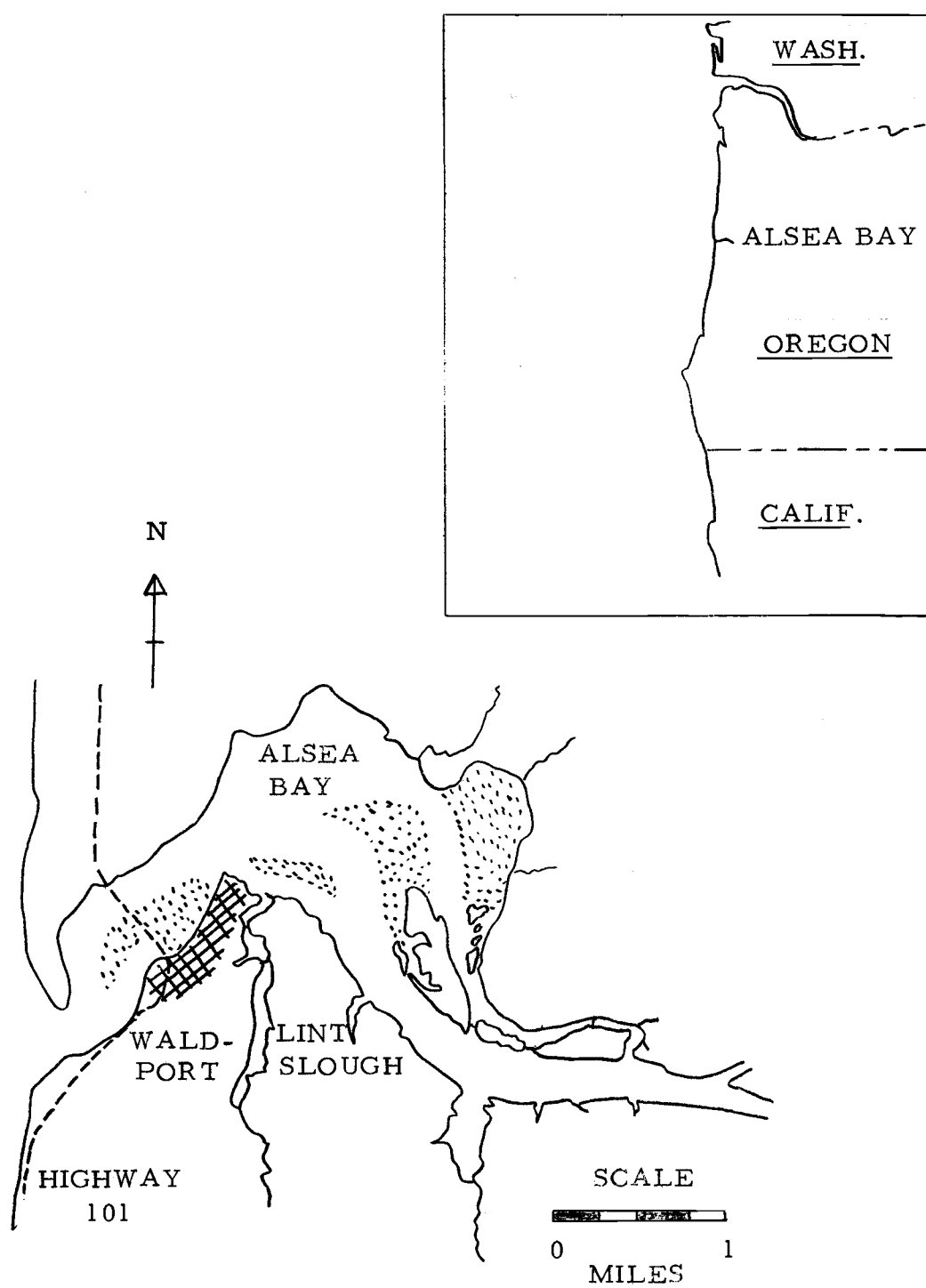
Figure 1. Alsea Bay, Waldport, Oregon

A bibliography of reports containing additional general information concerning the Alsea Estuary can be found in Appendix B.

Entrance Region

The entrance to Alsea Bay is a natural unimproved inlet, as shown in Figure 2. Depth over the outer bar of the inlet varies on a daily basis, however is generally less than five feet at MLLW. Navigation in the entrance region is extremely hazardous and should be attempted only by experienced personnel. The inlet is bounded on the north by a sand spit which seems to be reasonably stable, and on the south by a resistant sandstone-mudstone rock formation. This rock formation leads to quite irregular channel shapes in the narrower part of the inlet. The sand spit on the north seems to be composed of a layer of sand, below which is a layering of gravel and cobbles. The top surface of the cobble layer is about 4 to 5 feet below MLLW. The sand spit has been in its present location for as long as residents of the area can remember.

Net littoral transport in the area is southward, however seasonal variations are quite large. During the winter season transport is predominantly northward while during the summer the littoral drift is to the south. This leads to a frequent shifting of the offshore bar of the inlet, with the channel alignment varying from southwest to northwest during different times of the year.
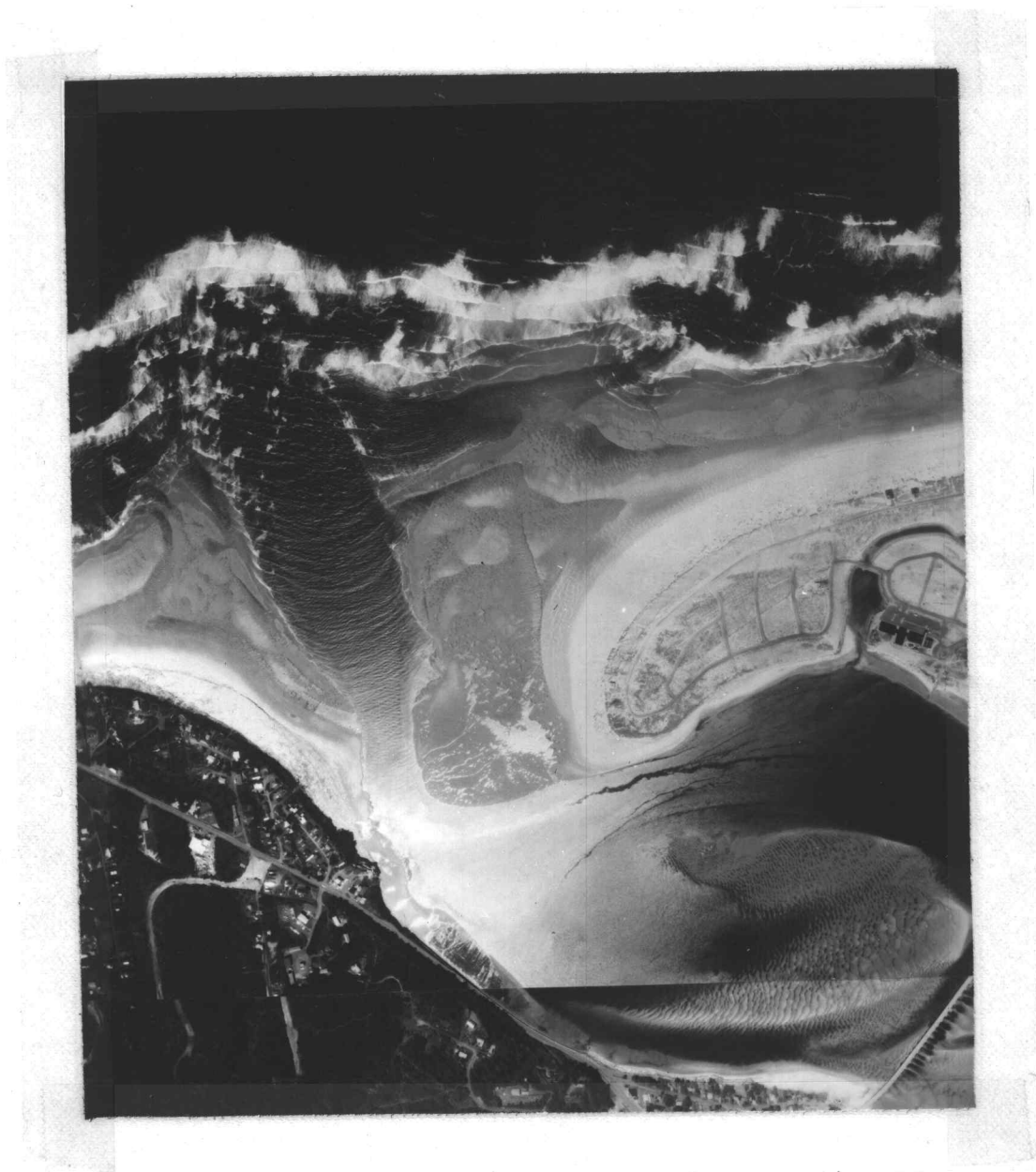
Figure 2. Photograph of Alsea Bay Entrance, May 1972

Width of the inlet at MLLW was 260 feet at the narrowest portion, and 850 feet near the outer bar, according to 1972 measurements. Minimum cross sectional area at MLLW was 5,570 square feet, occurring slightly seaward of the narrows. Length of the inlet from the bay to the outer bar is approximately 4800 feet.

IV. INFORMAL HISTORY OF EXPERIMENT

The first attempt to measure an estuarine discharge coefficient
at Alsea Bay occurred in January 1972. To measure the tidal height
on each side of the inlet it was proposed to place chain and float type
tide recorders atop six inch diameter aluminum stilling wells which
had been jetted into the sand. Additional support of the stilling wells
was to be provided by three guy wires fastened to six foot long fence
posts driven into the sand. These stilling wells were to be placed at
about the MLLW line on the beach, and could then be serviced at low
tide. This installation was attempted and it was found that the stilling
wells could not penetrate more than three to four feet into the sand,
instead of ten feet as planned, due to the presence of large cobbles.
However this depth was felt to be sufficient for support; the stilling
well installation was completed as planned. The following day
revealed that two of the three structures had failed, with the third
stilling well quite unstable. The reason for failure was that under
cyclic loading by wave action the fence posts used to anchor the guy
wires had tended to creep through the sand, until guy wire slack
allowed the stilling well structure to collapse.

Following this unsuccessful expedition, the Port of Alsea was
contacted concerning having piling driven at the necessary locations.
Stilling wells could be fastened to these piles and tidal measurements

obtained in this manner. The necessary construction permits to drive piling were obtained from the Corps of Engineers and the Coast Guard. Members of the Port of Alsea very generously offered to donate their time and services in the pile driving effort. In June 1972, three piles were placed in the entrance region on the north side of the inlet: one near the outer bar, one at the narrows, and one inside the inlet near the tip of the sand spit. Within two days the piling near the outer bar and at the narrows were removed by wave action. The pile near the inside tip of the sand spit remained serviceable and was used until the completion of the field work in July 1972.

From these experiences it was felt that to install a tide recording station near the outer bar would not be feasible. To solve this difficulty in obtaining ocean tide records, a submersible high resolution tide recorder was leased from Bass Engineering. This recorder was placed outside the outer bar in 90 feet of water. To obtain tide records at the inlet it was decided to place a chain and float tide recording station on the rock formation at the south side of the inlet. This was accomplished on July 10, 1972. An impact drill was used to drill holes in the mudstone, and rock bolts placed to anchor guy wires. A structure to support a stilling well was fabricated using three aluminum ladders, hose clamps, rope, and tape, as is shown in Figure 3. This structure proved

Figure 3. Alsea Entrance Tide Recorder, Station 2

quite successful and lasted the duration of the period of field meas-

urements.

V. TIDAL MEASUREMENTS

Tidal measurements for this study were required for at least

two locations: the ocean and the bay. In addition, in support of

general water circulation studies of Alsea Bay and its tributaries,

tidal records were obtained at seven other locations within the bay in

order to completely characterize the tidal response of the estuary.

Tidal records within the estuary were obtained with Type F Water

Level Recorders manufactured by Leupold and Stevens, Incorporated.

These are chain and float recorders requiring placement of a stilling

well and instrument platform, with servicing daily. From records

obtained with the Stevens Type F Recorder, tidal height may be

determined to within .03 feet, and time of occurrence to within 3

minutes. Ocean tide records were obtained with a submersible

pressure-sensitive instrument manufactured by Bass Engineering.

This instrument is self-contained and designed for water depths to

100 meters. Servicing of the instrument is required every 31 days for

replacement of batteries and chart paper. With the Bass Tide Gauge

tidal height may be determined to within .05 feet and time of occur-

rence to within 3 minutes.

Shown in Figure 4 are the locations of 1972 Alsea Bay tide

recording stations. In determination of an estuarine discharge

coefficient, of primary importance are tide records for the bay just

N

ALSEA
BAY

6

4

3

5

2

1
●
(Depth 90')

7

8

HIGHWAY
101

SCALE

0   1
MILES
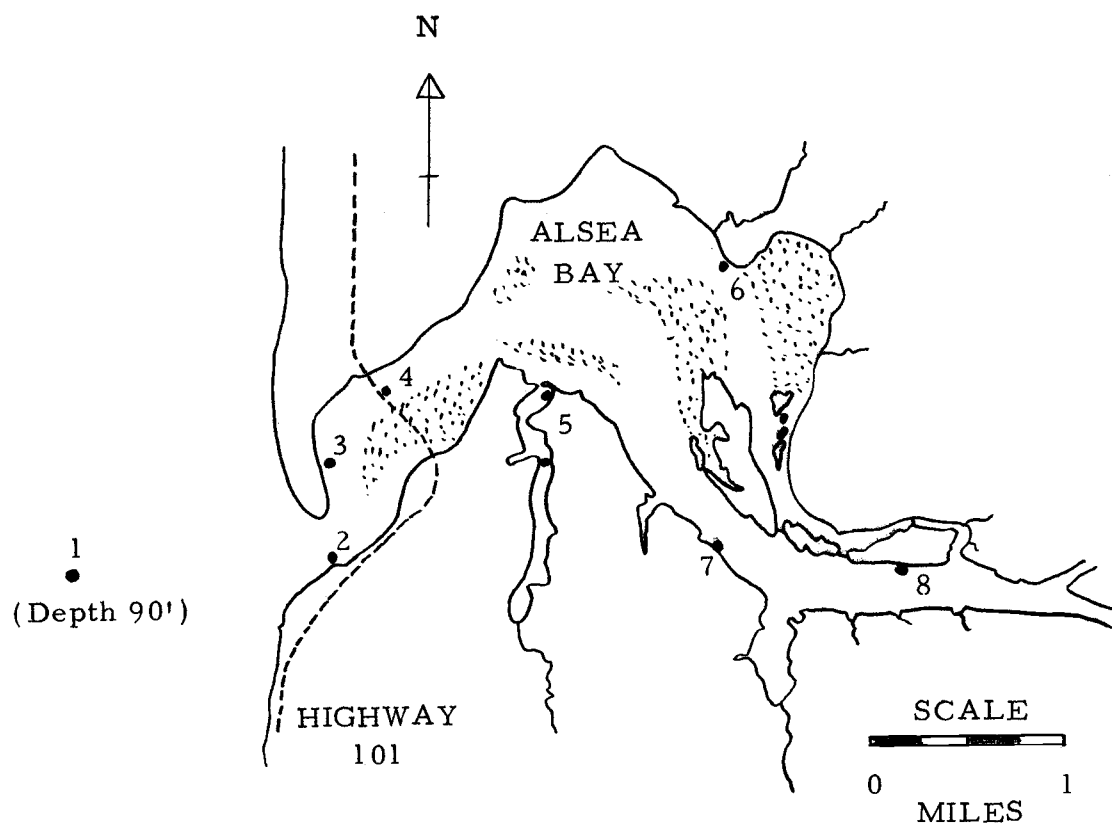
Figure 4.   Tide Recorder Locations, Alsea Bay, 1972

within the entrance and for the ocean. Since it was not certain

whether Station 2 adjacent to the mouth would show a tidal response

characteristic of the bay, or would instead reflect entrance effects,

tidal data from Station 3 on the bay side of the spit was also analyzed.

This section will examine the records of Stations 1, 2, and 3 in detail,

while the tidal response of the complete estuary is treated in Appendix

A.

It will be recalled that for the determination of a discharge

coefficient for the entrance, three parameters must be measured;

entrance shape, flow rate, and tidal height of the bay and ocean

relative to a reference level. For the tide recording stations within

the estuary, records were made relative to MSL, as established from

Coast and Geodetic Survey benchmarks. However, an absolute

reference level for the ocean tide record could not be determined due

to the difficulty of employing survey leveling techniques in the ocean.

In order to establish a common reference level between bay and ocean

tide records, it was initially assumed that the mean of high and low

waters during the same period of record for each station would be the

same elevation. This reference level was found to be 0. 32 feet

above MSL as established by the Coast and Geodetic Survey. Further

analysis, during determination of the head differential between the

ocean and the estuary found it necessary to shift the entrance tidal

curves upward by approximately 0. 2 feet relative to the ocean tidal

record. The criteria for this are discussed further in Chapter VIII of this thesis. Fresh water inflow to the estuary during this period was approximately 100 cfs and could account for part of this shift.

To obtain ocean tide records the Bass Tide Gauge was placed offshore in 90 feet of water utilizing a single point mooring. Heavy seas and a South to North current greater than one knot caused problems during submergence of the tide gauge which eventually led to acceptable records for only two and one half days. Satisfactory records were obtained from 1900 hours July 11th, to 900 hours July 14th, 1972.

The bay entrance tide recording station, Station 2, was established on July 10th, 1972. As mentioned before, stability was achieved with an open structure of triangular cross section fabricated from aluminum ladders and supported by guy wires fastened to rock bolts. A stilling well was placed within the ladder structure, with an instrument platform attached to the top of the stilling well. A photograph of this tide recording station is shown in Figure 3. As the entrance region is subject to strong currents and surf action, the station was observed for 36 hours to be certain of its stability before placement of the Type F recorder. Upon placement of the recorder, tide records were obtained for five days, July 12th through the 16th.

Table I lists the times of high and low tides for Stations 1, 2, and 3, and gives the water level heights relative to the reference level as computed from the period of record for each station.

Table I. Tidal Data, Stations 1, 2, and 3, Alsea Bay

Date (1972)	Time (PDT)			Height* (ft)		
	1	2	3	1	2	3
July 11	1917	--	--	-2. 17'	--	--
July 12	01·09	0112	--	4. 70	4. 50'	--
	0810	0821	--	-5.96	-5. 63	--
	1448	1449	--	3. 41	3. 20	--
	2005	2028	2035	-2.02	-1.64	-1. 55'
July 13	0200	--	0230	4.26	--	4. 20
	0840	0900	0910	-5. 55	-5. 30	-5. 22
	1519	1522	1602	3. 68	3. 30	3.18
	2058	2107	2122	-1.98	-1.83	-1.85
July 14	0250	0256	0325	3. 74	3. 38	3. 28
	0920	0947	--	-4. 70	-4. 72	--

*relative to 0. 32 feet above MSL, or 3. 72 feet above MLLW.

The entrance discharge coefficient was to be determined during both flood and ebb flows. To make meaningful comparisons, it was felt to be desirable to analyze similar flow rates on the flood and ebb tides. Therefore, flow rates were measured for flood and ebb tides on successive days, July 13th and July 14th. Tidal ranges for these days were similar, with the ocean tidal range for the flood tide of July 13th being 9.23 feet, while the ocean tidal range for the ebb tide of July 14th was 8.44 feet.

Shown in Figures 5 and 6 are the tidal curves for Stations 1 and 2, as determined from records obtained at the bay entrance station and the ocean site. Tidal heights are given relative to MLLW as established by the U.S. Coast and Geodetic Survey, with the height of the ocean tide curves determined by the mean of high and low waters for the period of record, as discussed previously. Station 3 did not have a complete record for July 14th, however data from Station 3 are discussed further in Chapter VIII of this report.
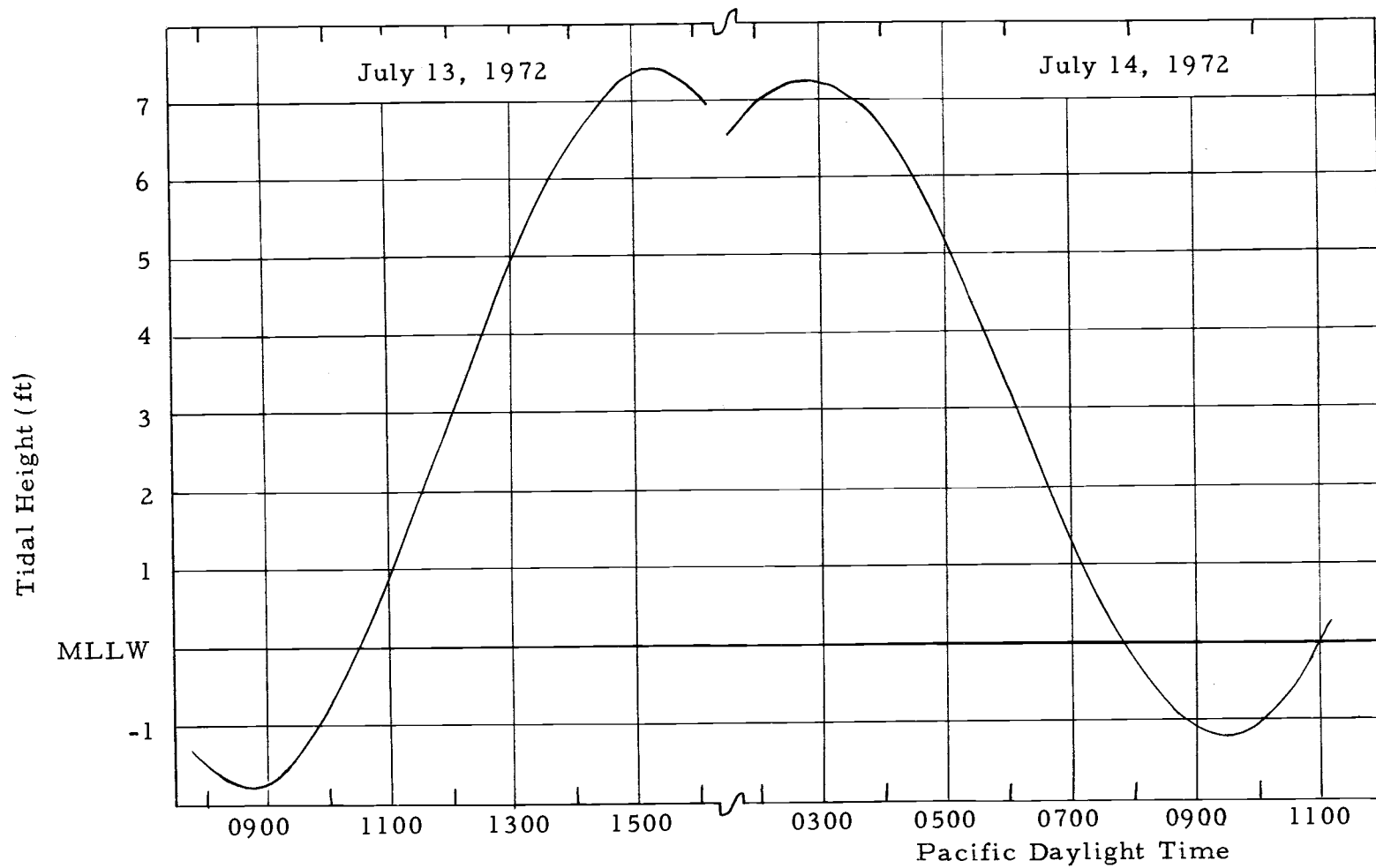
Figure 5. Ocean Tidal Curves, July 13 and 14, 1972
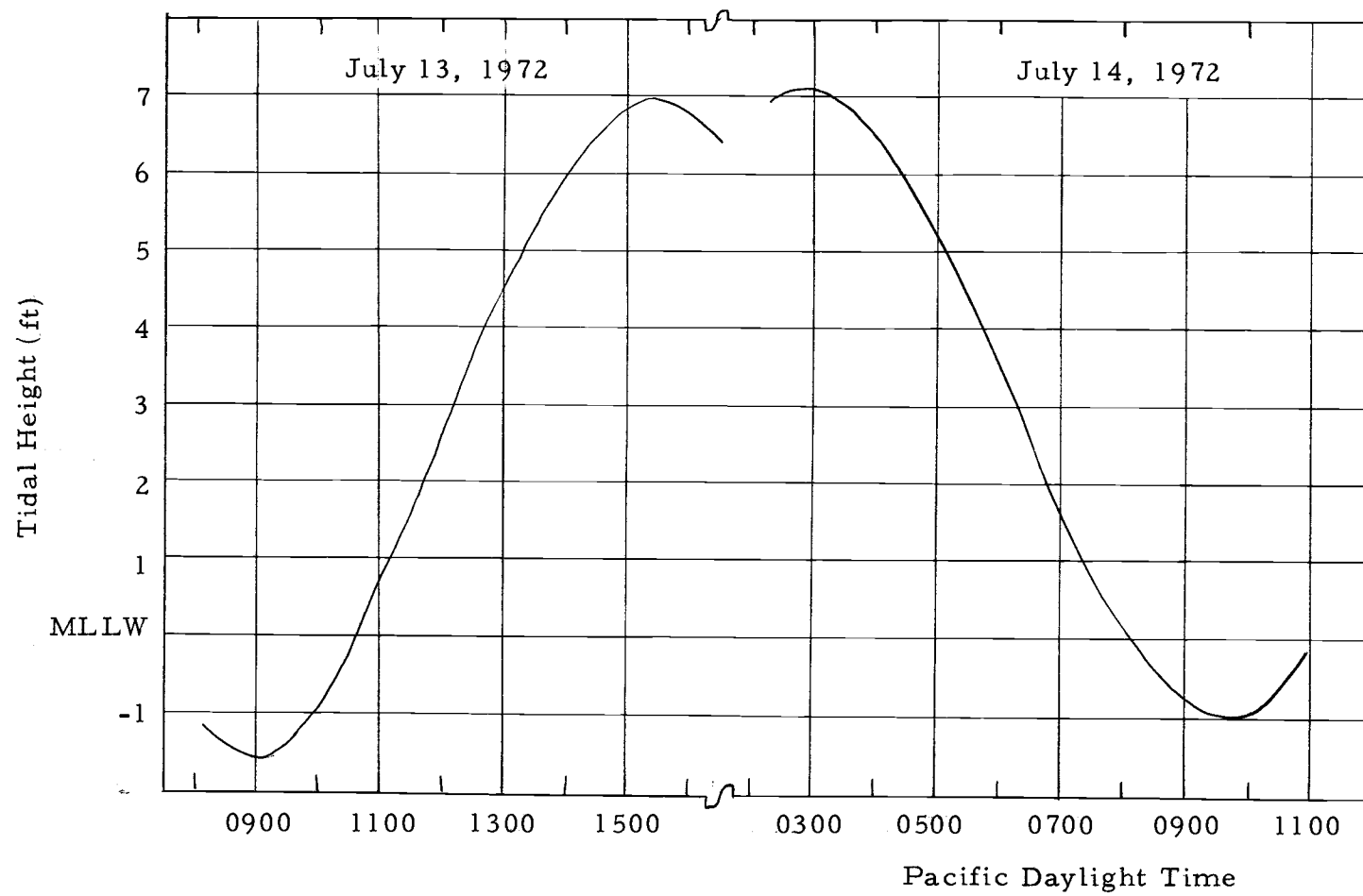
Figure 6. Alsea Entrance Tidal Curves, July 13 and 14, 1972

VI. FLOW RATES

To determine the flow rate of water through the Alsea entrance, eight current measurement stations were monitored during flood tide on July 13th, and ebb tide on July 14th, 1972. The positions of these current measurement stations were chosen to be on a semicircle within the entrance, normal to the direction of flow, as shown in Figure 7.

The rationale behind the choice of these positions was based on a combination of experience and current measurement limitations. Although the narrowest part of the entrance would be a logical section for determining flow rate, experience indicated that this region has quite irregular flows due to the unusual cross sectional shape creating eddy currents. The undercut bank on the south side of the entrance is the deepest portion of the entrance and not a feasible place to make measurements. Seaward of the narrows the channel shape becomes more uniform, however wave activity would make measurements uncertain and hazardous.

Velocity measurements were made using Price-type Gurley Salt Water current meters operated from 16 foot open aluminum boats. Measurements were begun at or near slack water and continued until the following slack current or reversal. Shown in Figures 8 and 9 are plots of velocity vs. time for each current measurement station.

Several interesting current flow patterns occur bayward of

WALDPORT

•8

7
•6
5
4
•3
•2
•1

ALSEA
BAY

g

g

e
e

d
d

c
c

b
b

a
a

NORTH

OFFSHORE BAR

OCEAN
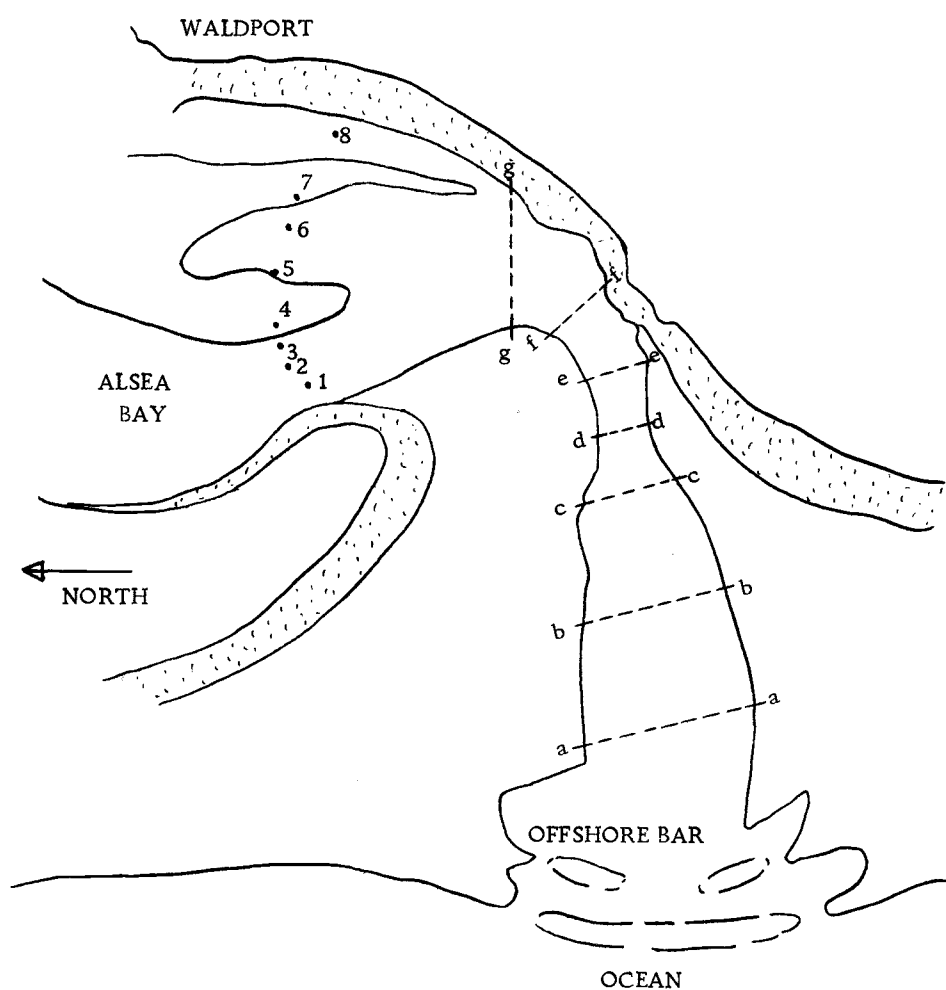
Figure 7. Current Measurement Stations and Bathymetry Profiles, Alsea Bay, 1972

Flood Tide, July 13, 1972
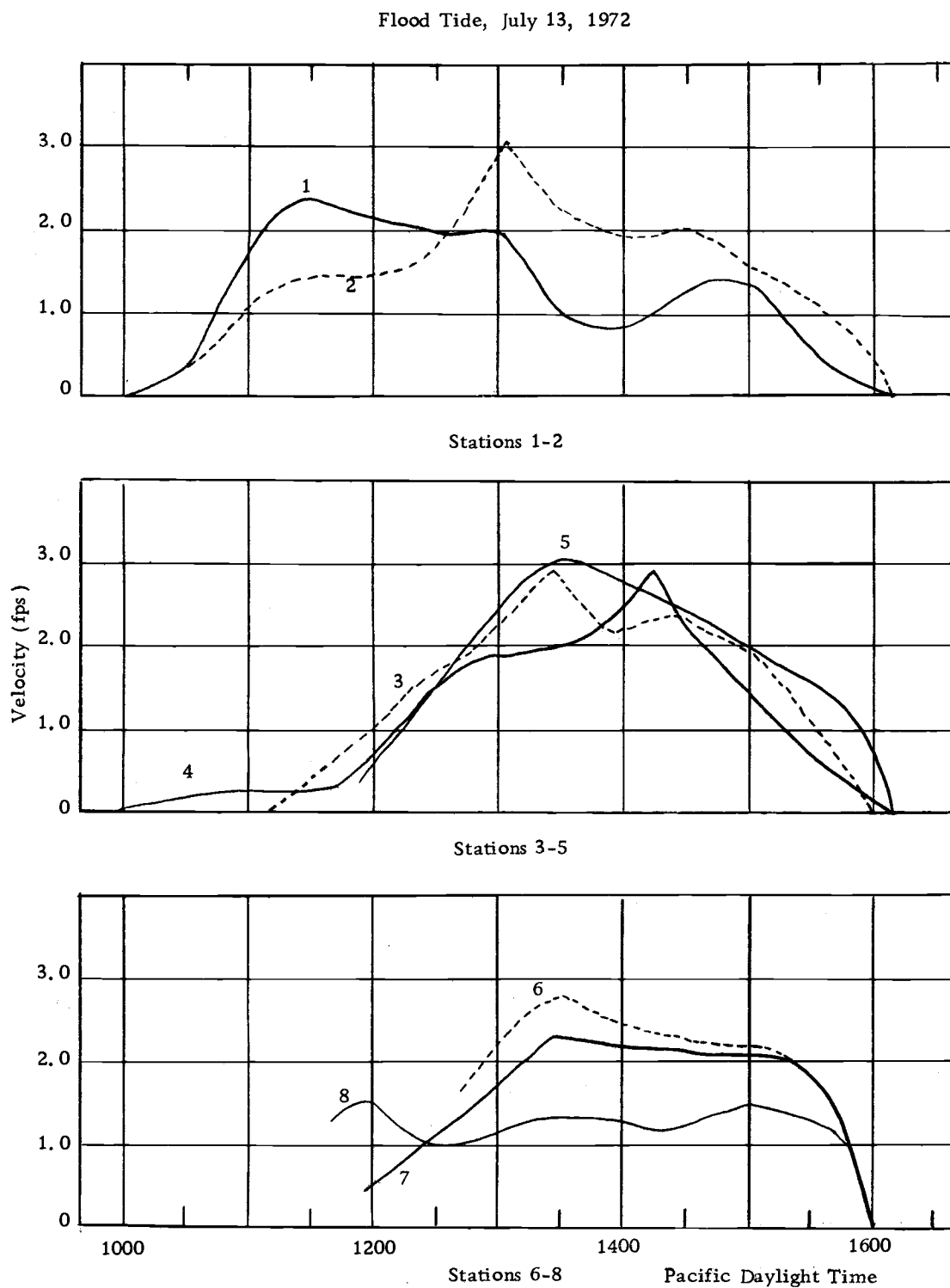
Figure 8. Flood Tide Velocity Measurements, Alsea Bay

Ebb Tide, July 14, 1972
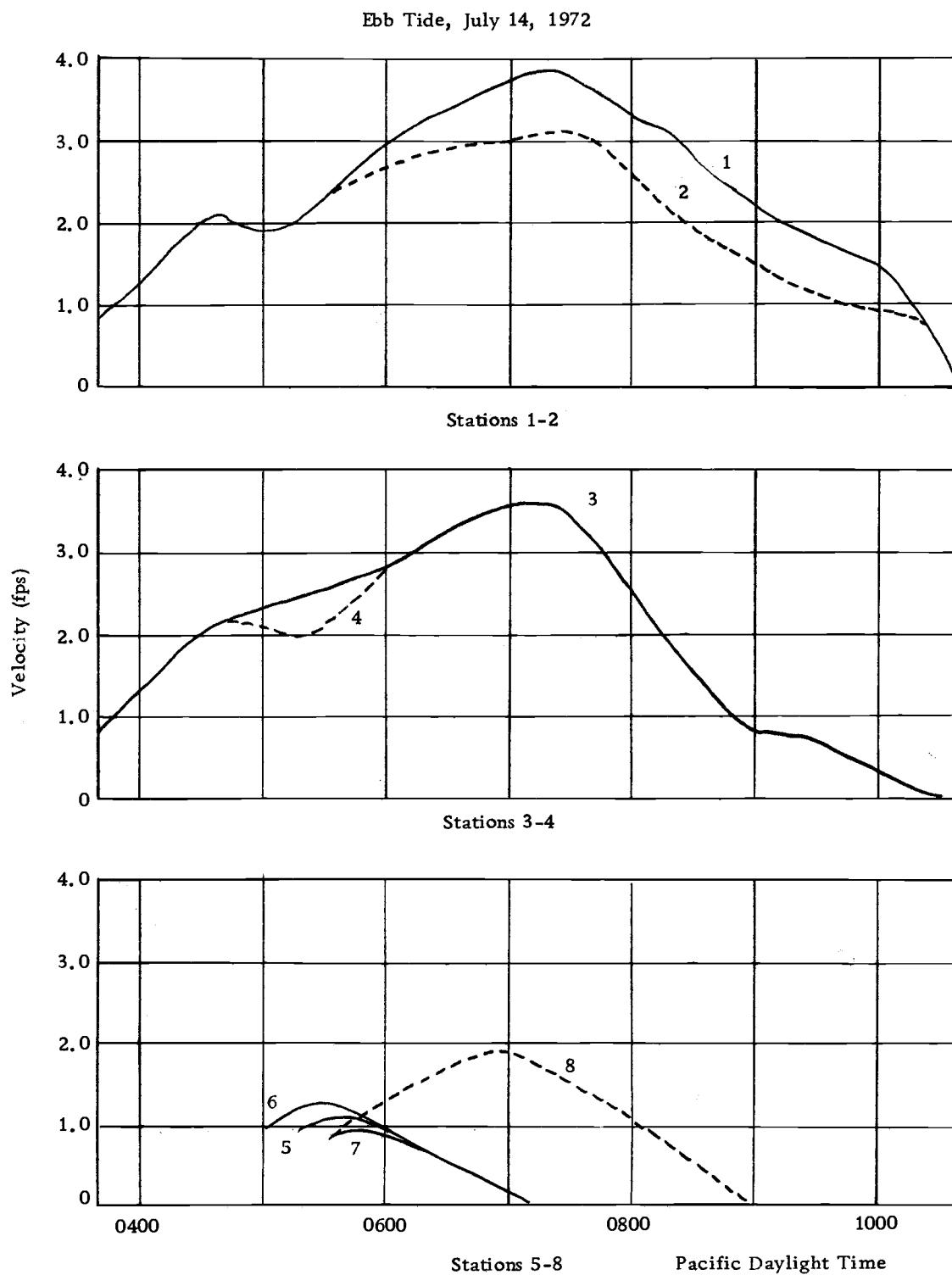
Figure 9. Ebb Tide Velocity Measurements, Alsea Bay

the inlet. During the early stages of a flooding tide the incoming

flow is deflected by the opposing sand flats after passing through the

entrance, and flows north along the spit before passing under the

Waldport Bridge. As the water height increases and the opposing

sand flats along the south side of the bay become covered, flows tend

to proceed across the sand flats, instead of being deflected, and

proceed under the bridge in a north-east direction. This flood cur-

rent pattern is illustrated in Figure 10. During ebb flows, the major-

ity of water tends to follow the main channel under the bridge and along

the spit, regardless of tidal stage. The only water flowing out of the

south side seems to be draining off of the immediately adjacent tidal

flats. Figure 11 illustrates ebb flow currents.

On July 15th, 1972, the cross sectional area of the current

measurement semicircle was determined using lead line soundings

and surveying techniques. The profile of this semicircle is shown in

Figure 12. The total flow rate was found by determining the flow

area for each current measurement station at various tidal stages

and multiplying by the measured velocity, then summing for the entire

cross section. Flow rate vs. time for this section is shown in Figure

13. It should be remembered these are not successive flood and ebb

tides, but tides which occur on successive days. As discussed previ-

ously, successive tides were not studied due to the nature of the

semidiural tides for the Pacific Northwest and the desire to consider

WALDPORT

HIGHWAY
101

ALSEA BAY

NORTH

OCEAN
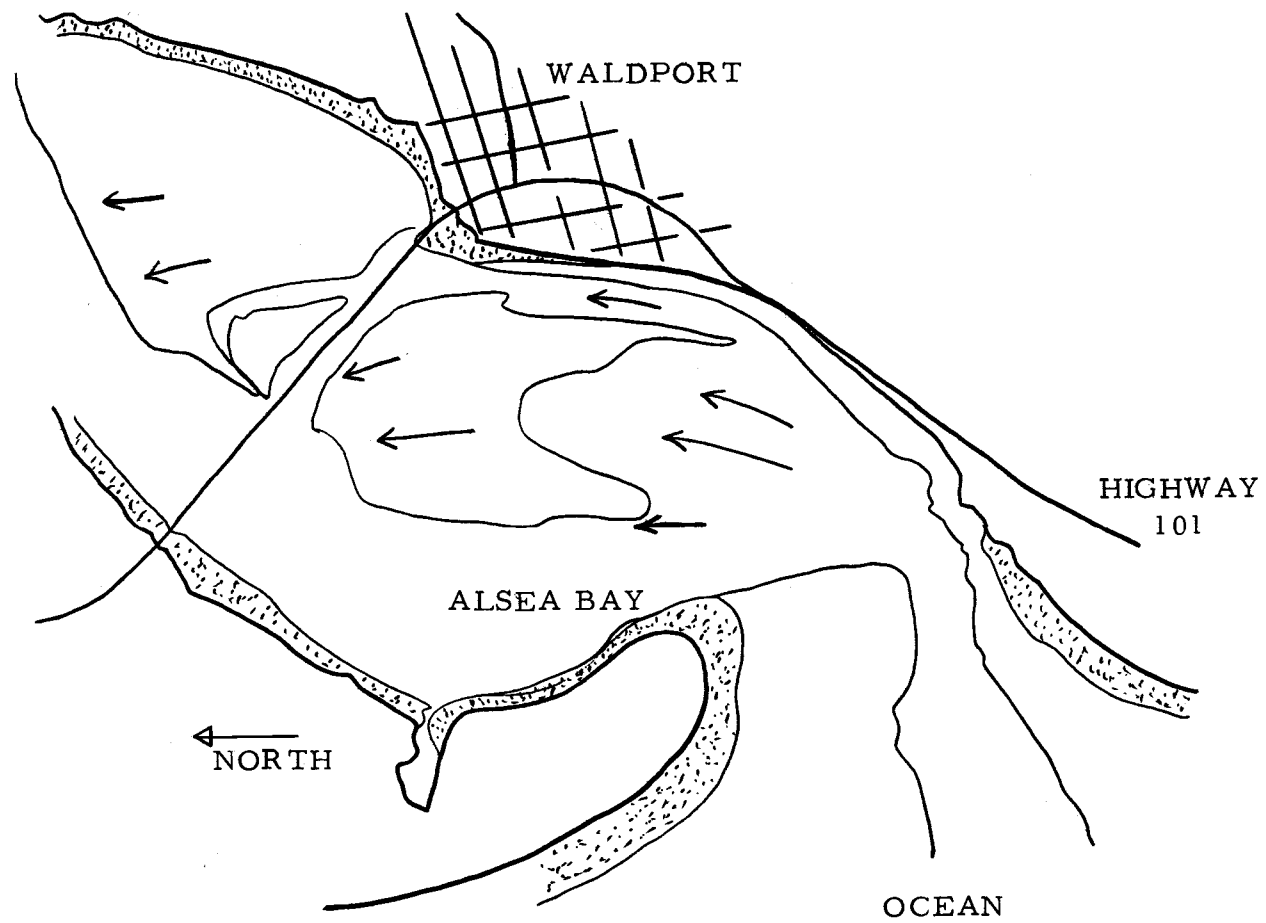
Figure 10. Flood Tide Flow Patterns, Alsea Bay

WALDPORT

(sand
flat)

ALSEA BAY

HIGHWAY
101

NORTH

OCEAN
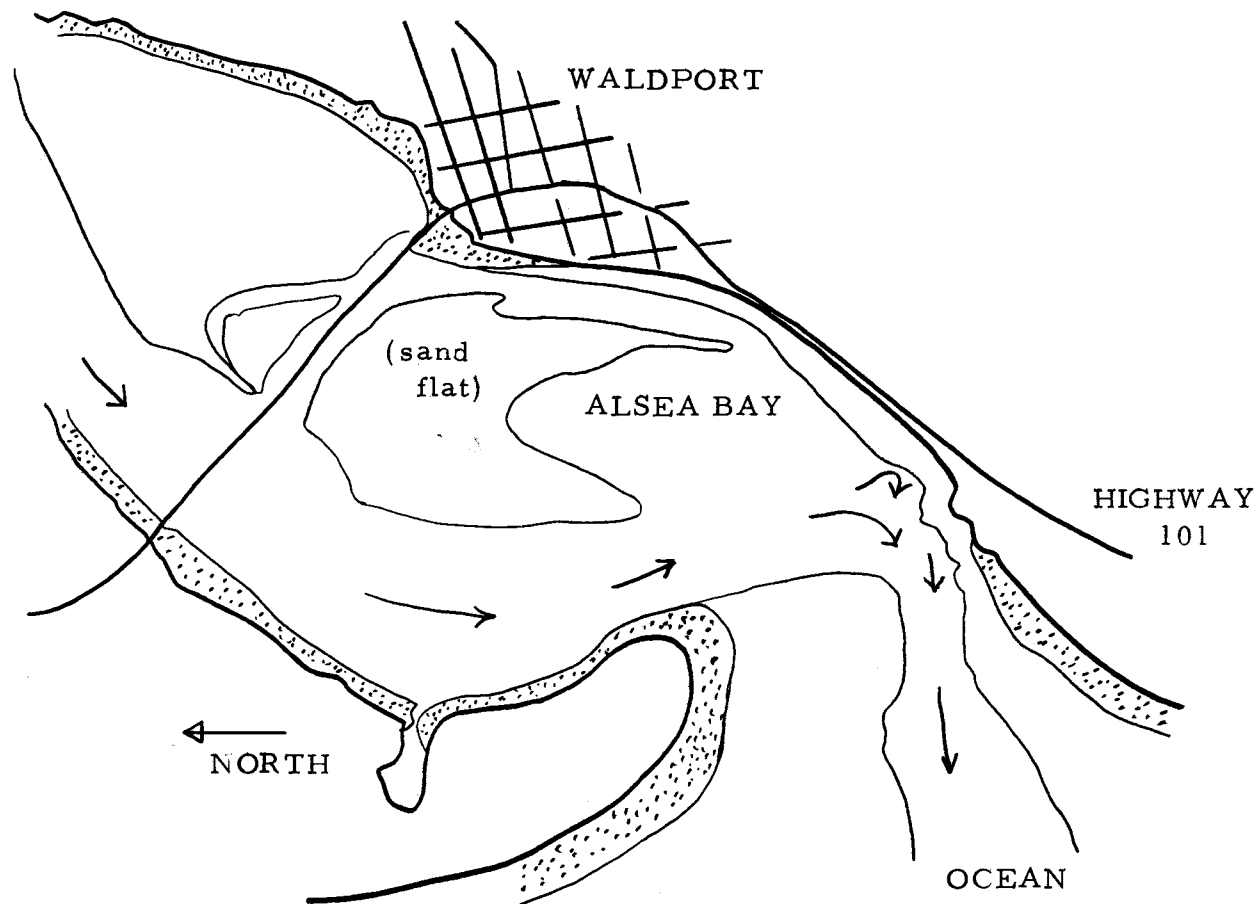
Figure 11.   Ebb Tide Flow Patterns, Alsea Bay
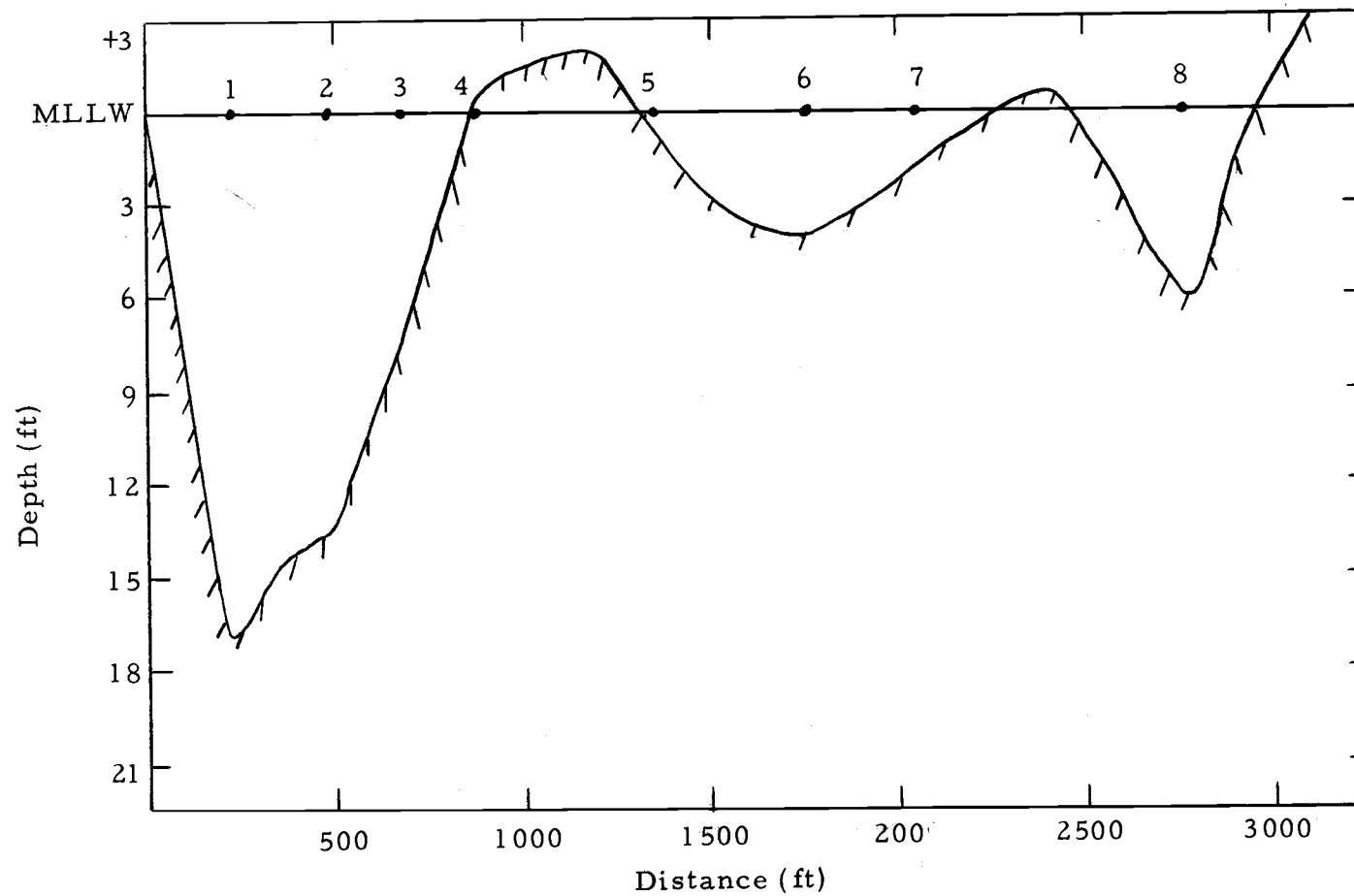
Figure 12.   Bathymetry Profile at Current Measurement Stations, Alsea Bay
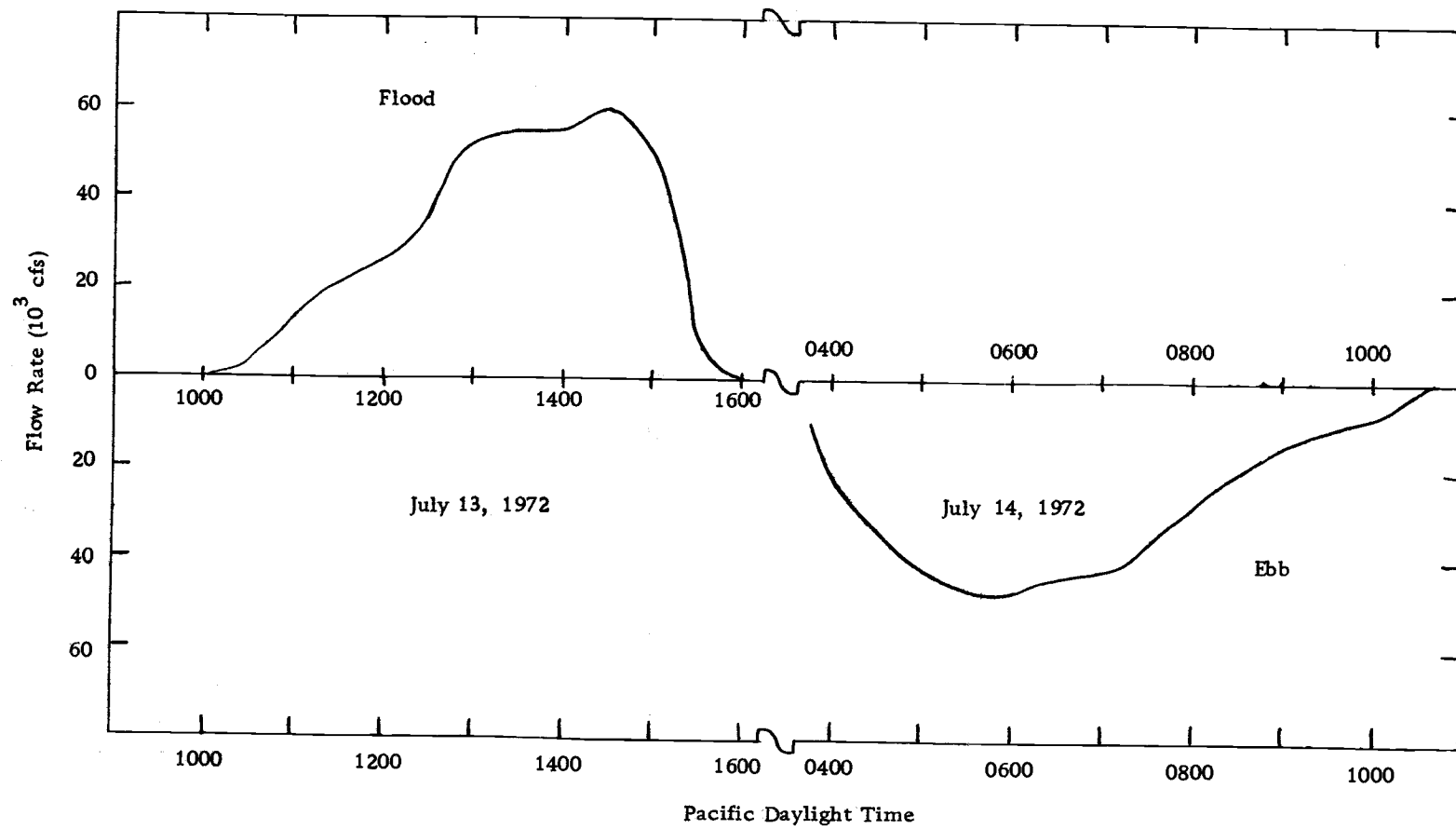
Figure 13. Alsea Bay Tidal Flow Rates, July 13 and 14, 1972

nearly equal flow rates for flood and ebb conditions.

Though the plot of flow rate vs. time roughly resembles a sine curve, as one would expect, it is somewhat irregular. This irregularity is due to the characteristics of the Alsea estuary. As tidal stage increases and a particular section of the tidal flats in the bay becomes covered, a sudden increase in the surface area of the bay occurs. This sudden increase in the bay area results in increased flow rates, and for a small estuary this effect may be felt back to the entrance and results in temporarily higher flow rates. This is most noticeable on the flooding tide.

VII. ENTRANCE SHAPE

Bathymetry measurements at several sections across the entrance to Alsea Bay were made on July 12, 1972. Depths were measured using a sounding line and a fathometer, both being accurate to the nearest foot. The positions of soudings were determined by triangulation from two shore-based transits. Craft available were 16 foot open aluminum boats, from which the majority of measurements were made, and a 22 foot Calkins Bartender for surf operations.

Figure 14 shows the positions of the cross sectional profiles, and gives a rough idea of channel shape. Figures 15, 16, 17, and 18 give correspondingly more detailed information on these profiles. Depths given are referenced to MLLW, as established by Goodwin (1970) to be 3.42 feet below MSL for Alsea Bay. The cross sectional area, width, and maximum depth for each profile is given in Table II.

Table II. Entrance Shape Information, Alsea Bay

Profile	Maximum Depth (ft)	Width (ft)	Cross-Sectional Area (ft^2)	Hydraulic Radius (ft)
a-a	8.4	1,010	9,000	6.7
b-b	9.8	600	5,570	8.9
c-c	18.0	295	5,850	18.3
d-d	29.5	260	5,940	22
e-e	27.5	280	6,390	22.5
f-f	44.0	365	11,000	27
g-g	11.2	860	8,700	10

WALDPORT

●8

●7

●6

●5

●4

●3
●2
●1

ALSEA
BAY

g   f

e→

e→

d→

c→

b→

a→

NORTH

Scale: (Approx.)
1" = 10³ feet (±10%)

OFF SHORE BAR

OCEAN
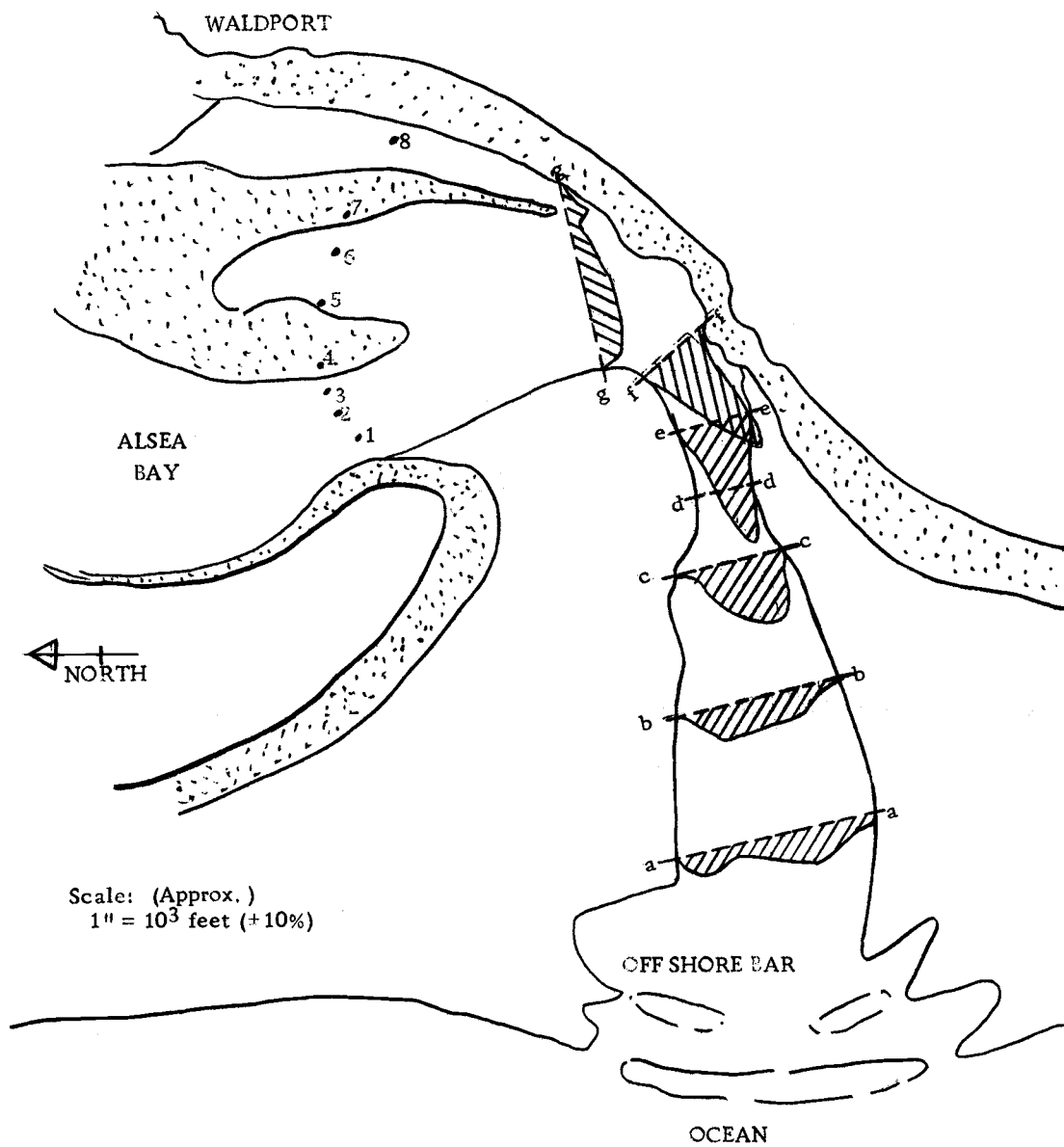
Figure 14, Illustrative Drawing of Entrance Shape, July 12, 1972
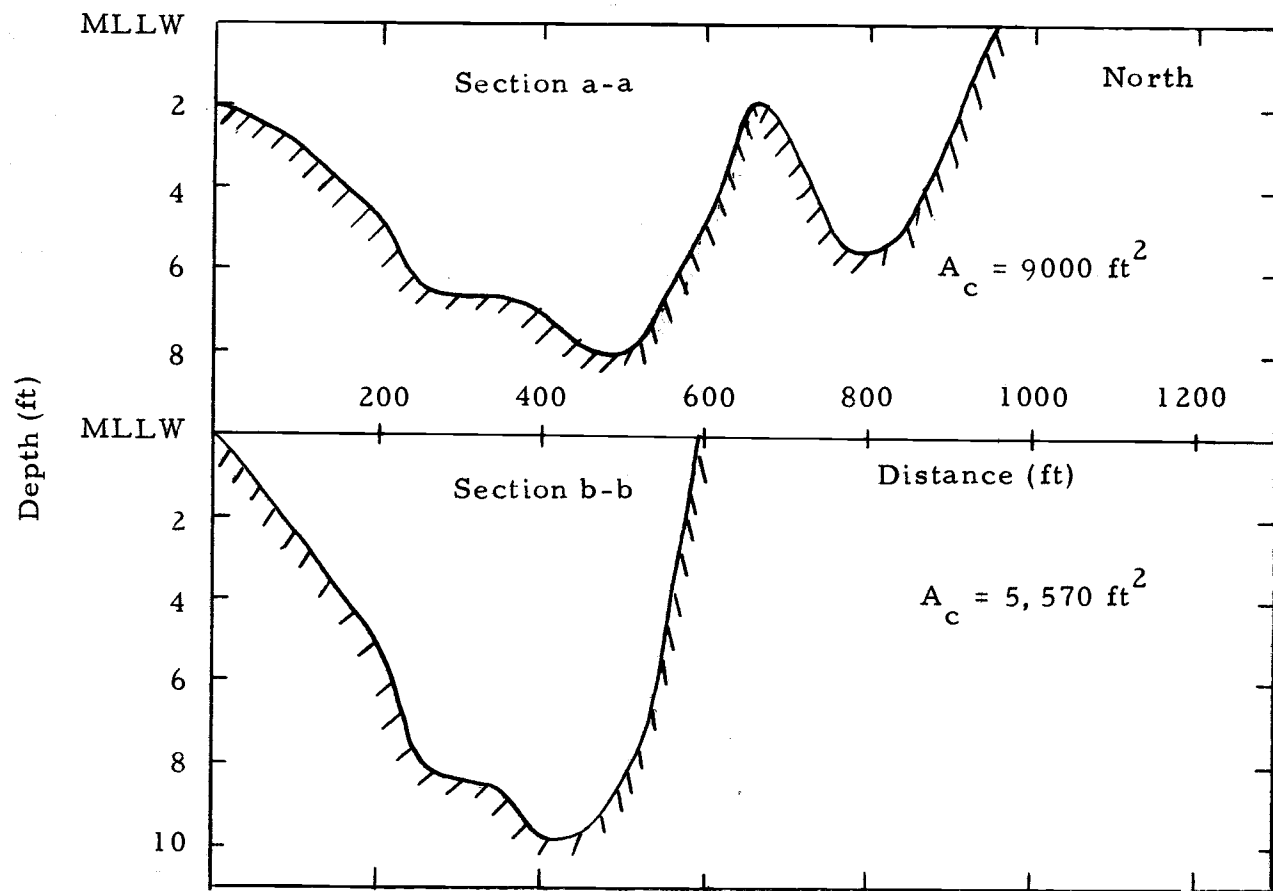
Figure 15.   Alsea Bay Bathymetry Profiles,   Sections a-a and b-b,   July 1972
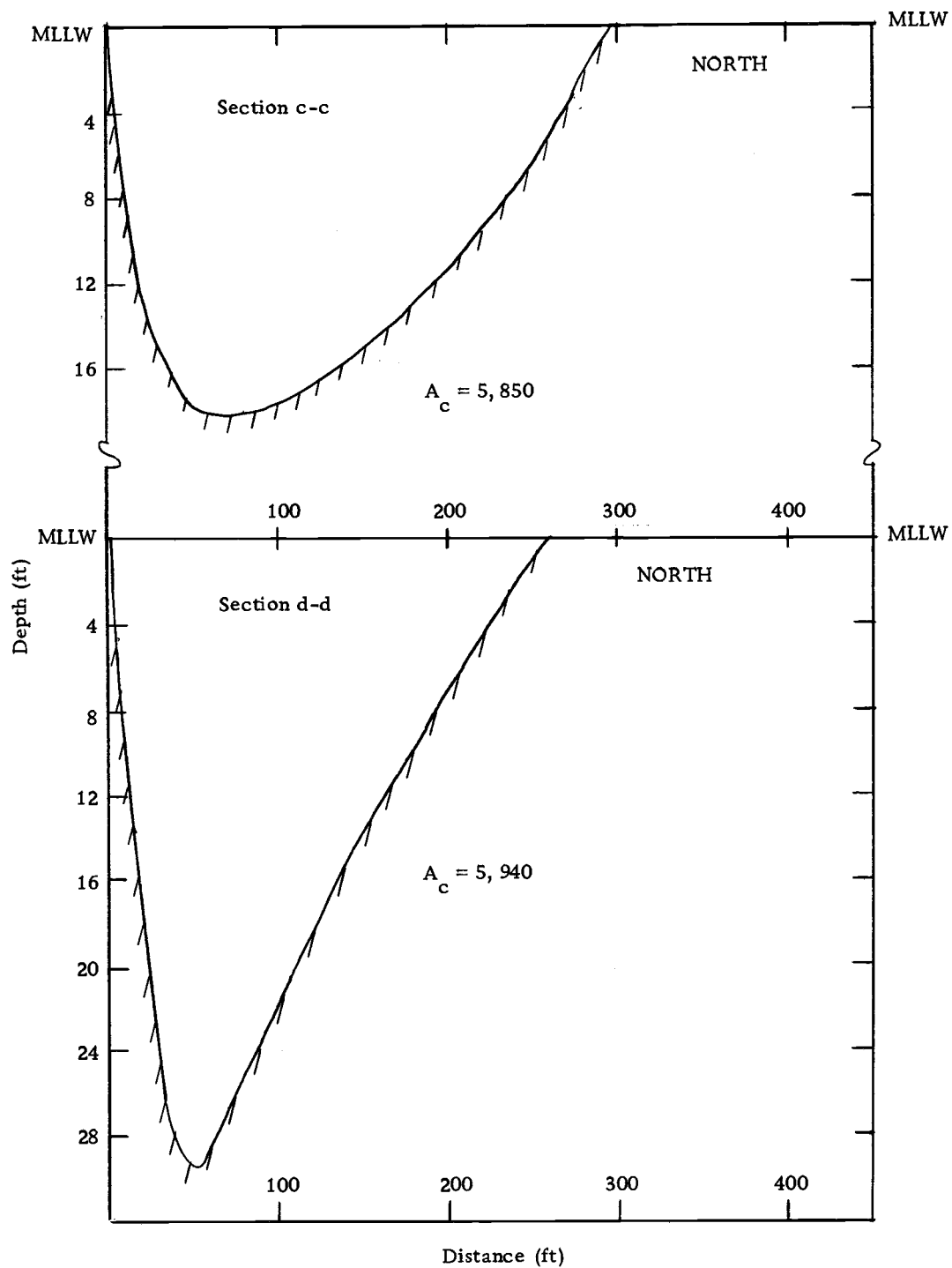
Figure 16. Alsea Bay Bathymetry Profiles, Sections c-c and d-d, July 1972
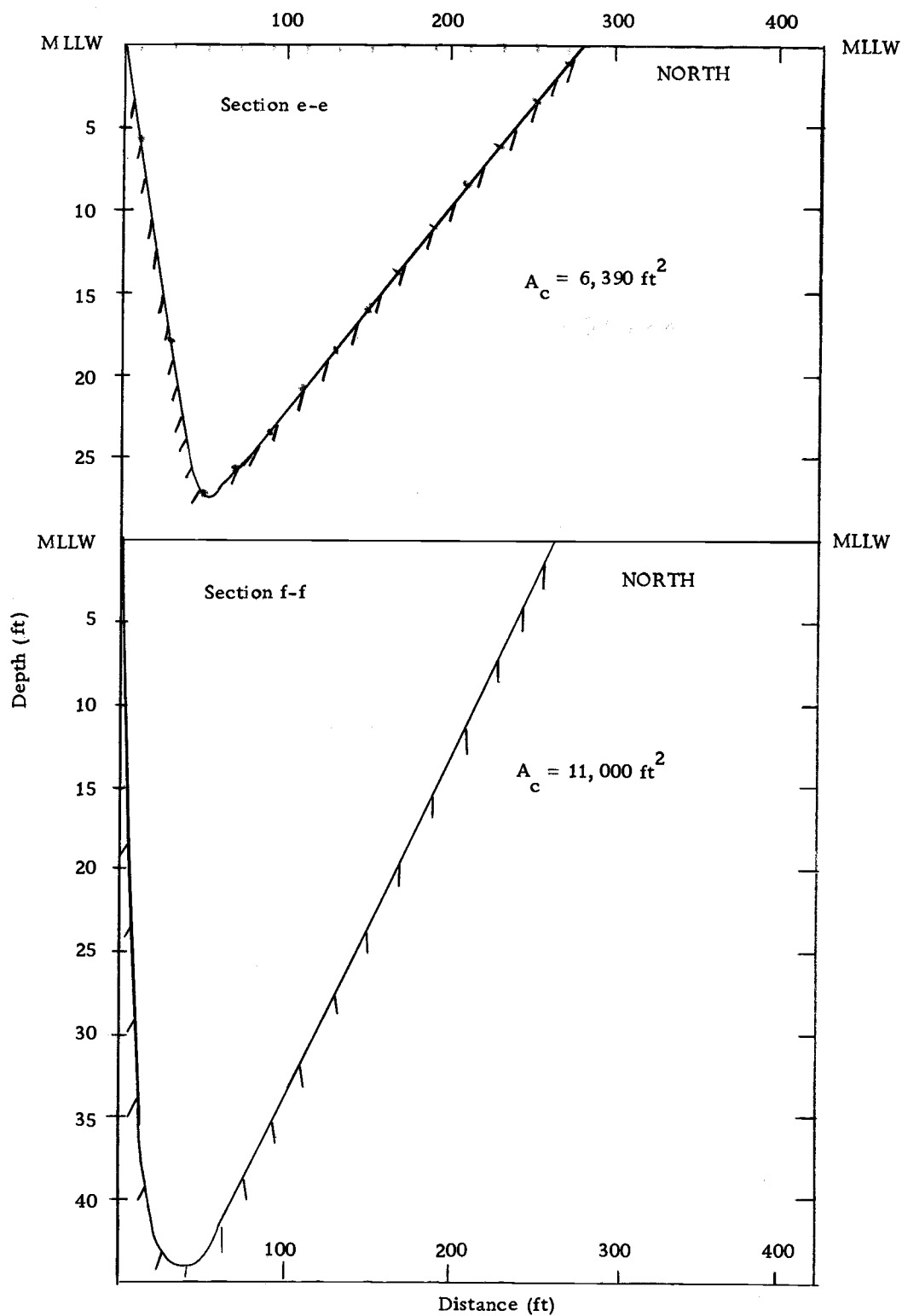
Figure 17. Alsea Bay Bathymetry Profiles, Sections 3-3 and f-f, July 1972
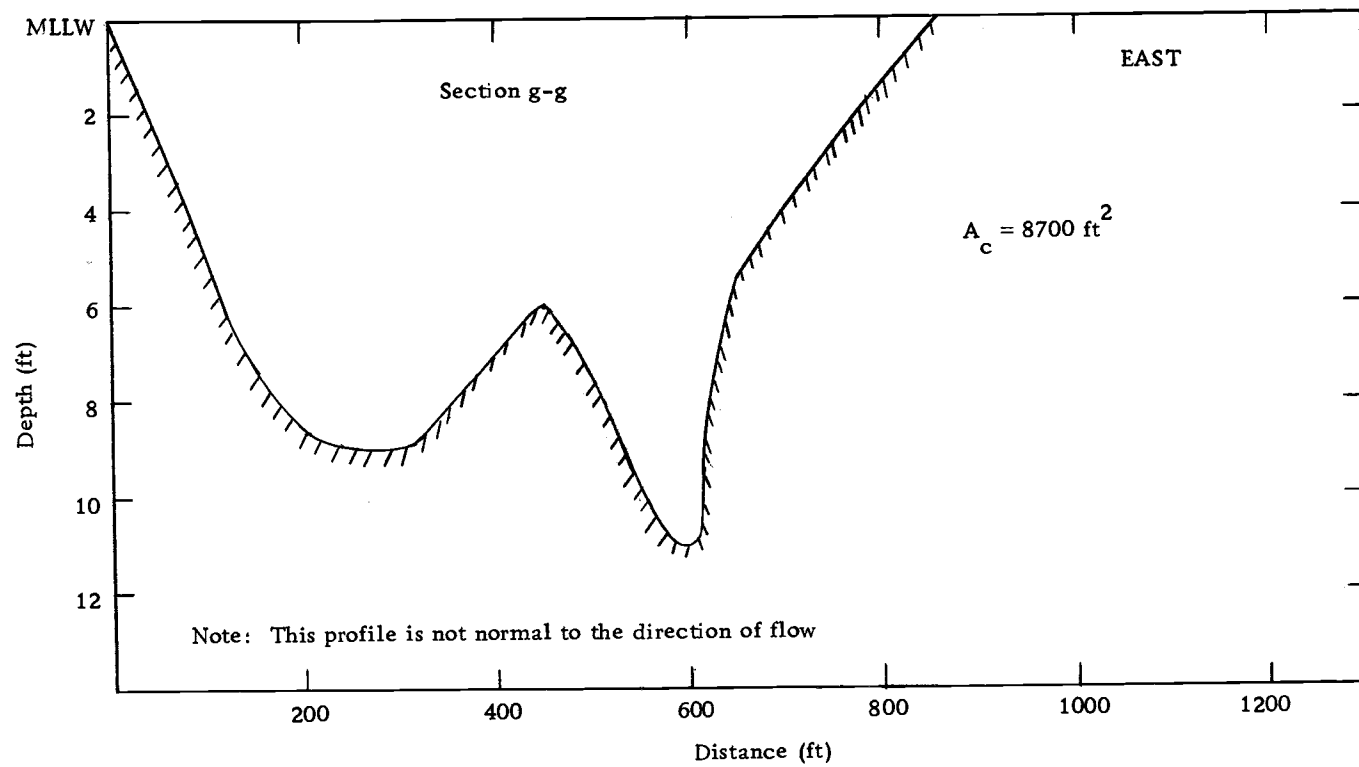
Figure 18. Alsea Bay Bathymetry Profile, Section g-g, July 1972

In addition to the cross sectional profiles, a longitudinal profile of the inlet was obtained. This was run on the centerline of the channel, and is shown in Figure 19. Maximum depth of the centerline of the inlet is 30 feet, and minimum depth is less than five feet at MLLW. The length of the entrance channel is nearly one mile.
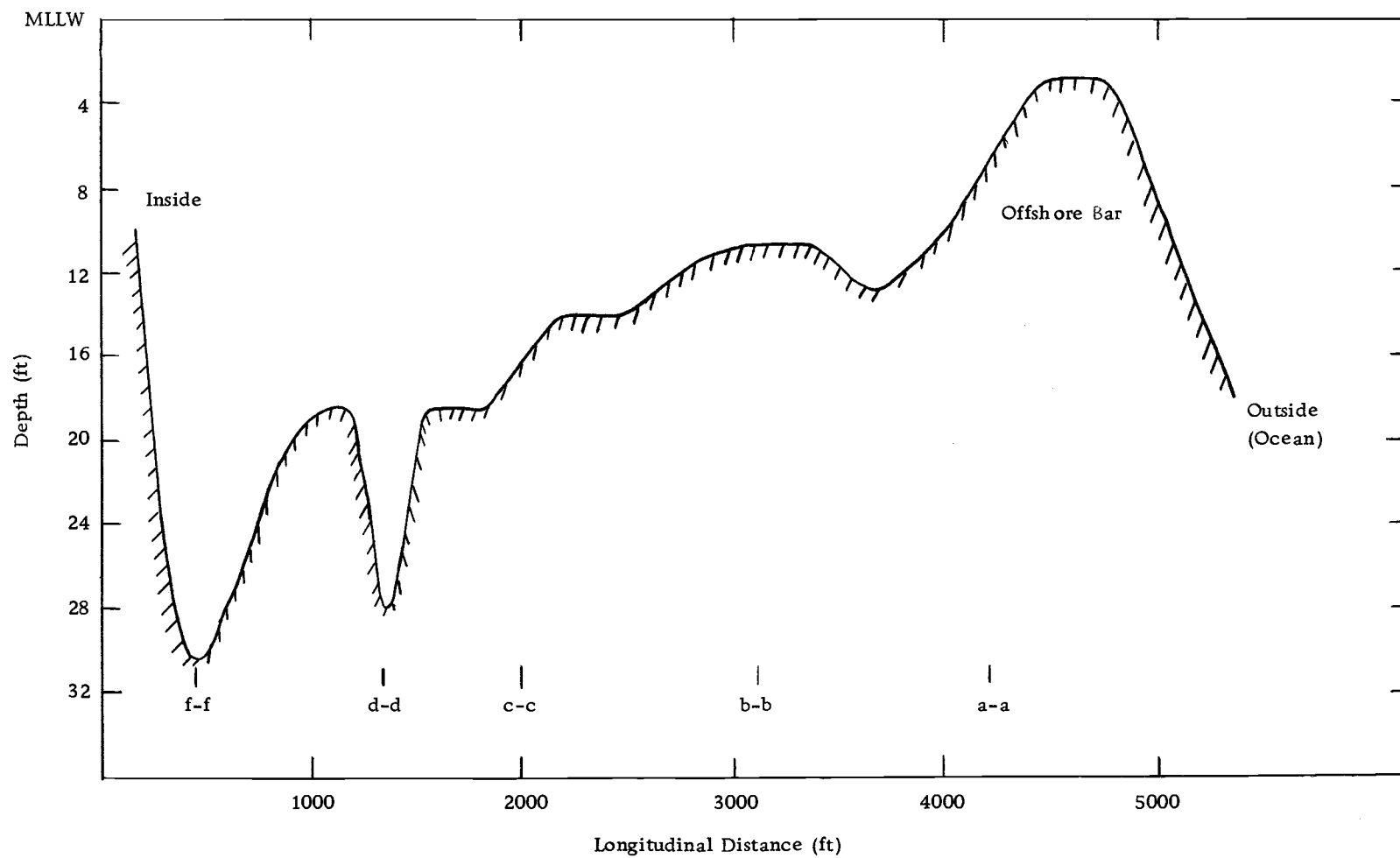
Figure 19. Longitudinal Profile of Alsea Bay Entrance Channel, 1972

VIII. ANALYSIS

Determination of Discharge Coefficient C

The most sensitive parameter affecting the determination of

an entrance discharge coefficient for Alsea Bay is the water height

differential across the inlet, as determined from tidal records of the

ocean and bay. To achieve the proper relationship between the ocean

and bay tide records, hydraulic considerations would indicate several

criteria should be satisfied.

1. When the ocean and entrance tidal curves cross is a time

    zero head differential exists across the inlet, or $\Delta h = 0$. This

    time should correspond to the periods of slack water.

2. If the cross sectional area or flow area of the inlet remains

    constant, maximum flow rates should occur concurrently

    with maximum head across the inlet. However, since the

    flow area of the inlet changes with tidal stage this will affect

    the time of maximum flow.

Before applying these criteria to analysis of the tidal relation-

ships between ocean and bay, some comments should be made. First,

during tidal data collection, the chain and float recorders used within

the bay required daily servicing to change charts and wind the clock

mechanism. As each chart is changed and the pen reset, the time

must be noted on the chart. Due to several ongoing research projects on Alsea Bay during the period of this study, different personnel were changing the recorder charts each day, unfortunately without the synchronizing of wrist watches. Thus an error in time of several minutes for each record is possible. It may be necessary to shift the bay tidal curves forward or back to account for this error. Second, since it was not possible to employ surveying techniques to establish a common reference level for ocean and bay tide recorders, it was assumed that the mean of high and low waters for each station would correspond to a common reference elevation. This assumption is not necessarily valid, due to fresh water inflow to the bay. One would expect the mean elevation within the bay to be greater than the mean elevation of the ocean.

Flood Tide Analysis

From hydraulic considerations, the relationships between tidal curves for Stations 1 and 2 were established as shown in Figure 20. For the flood tide of July 13, the relationship shown in Figure 20 was achieved by moving the bay entrance tidal curve up by .22 feet, and ahead by 2 minutes. This satisfactorily results in zero head differential across the inlet occurring at times of slack water, with maximum flow occurring at the same time as the maximum head differential.
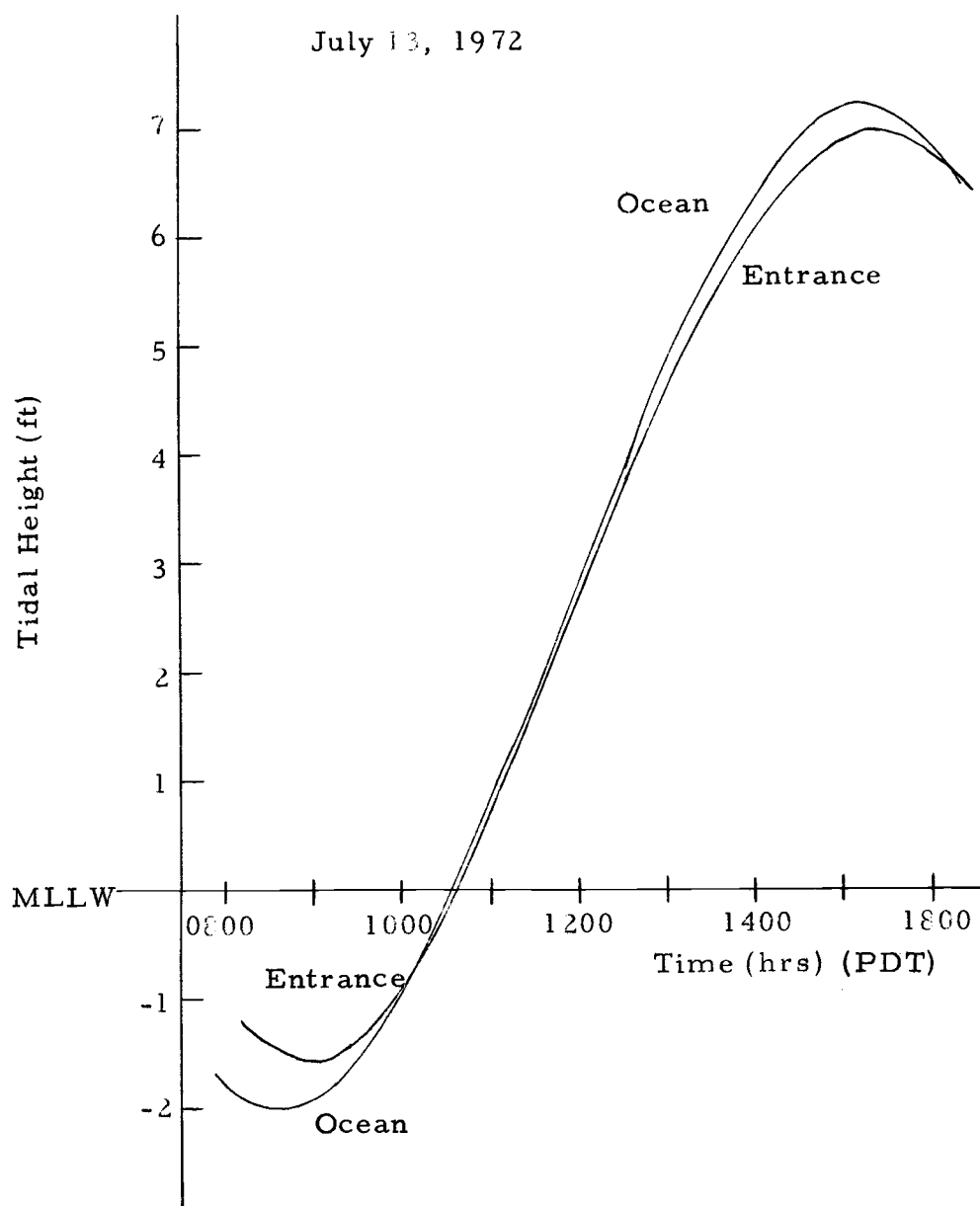
Figure 20. Tidal Relationship Between Stations 1 and 2,
Alsea Bay, July 13, 1972

Calculations to determine a discharge coefficient C from these Δh_{1-2} values indicated insufficient head existed across the inlet to account for the measured flow rates. One possible explanation for this discrepancy is the tidal response at Station 2 was affected by the inflowing jet and was not representative of the tidal response of the bay.

To determine the validity of this explanation, the relationship between tidal Stations 2 and 3 must be examined. Station 3 is bayward of the spit and would not be affected by the inflowing jet. A tracing (reduced) of the tidal records for these stations is shown in Figure 21. By adding the tidal height difference between Stations 2 and 3 to the tidal height difference between Stations 1 and 2, the height differential between the bay and ocean, Δh_{1-3}, was determined. The relationship between Δh_{1-3} and Q is shown in Figure 22.

Considering the parameters requiring field measurement in the relationship

$$Q = C A_c \sqrt{2g \, \Delta h,}$$

the only parameter yet to be accurately determined is the cross sectional area of the inlet as a function of tidal stage. The question arises as to which part of the inlet should be measured to determine this area. In the fluid mechanics of fluid flow meters for determining the discharge coefficient of a nozzle, the cross sectional area of the throat is used. Similarly, for an estuary entrance the cross
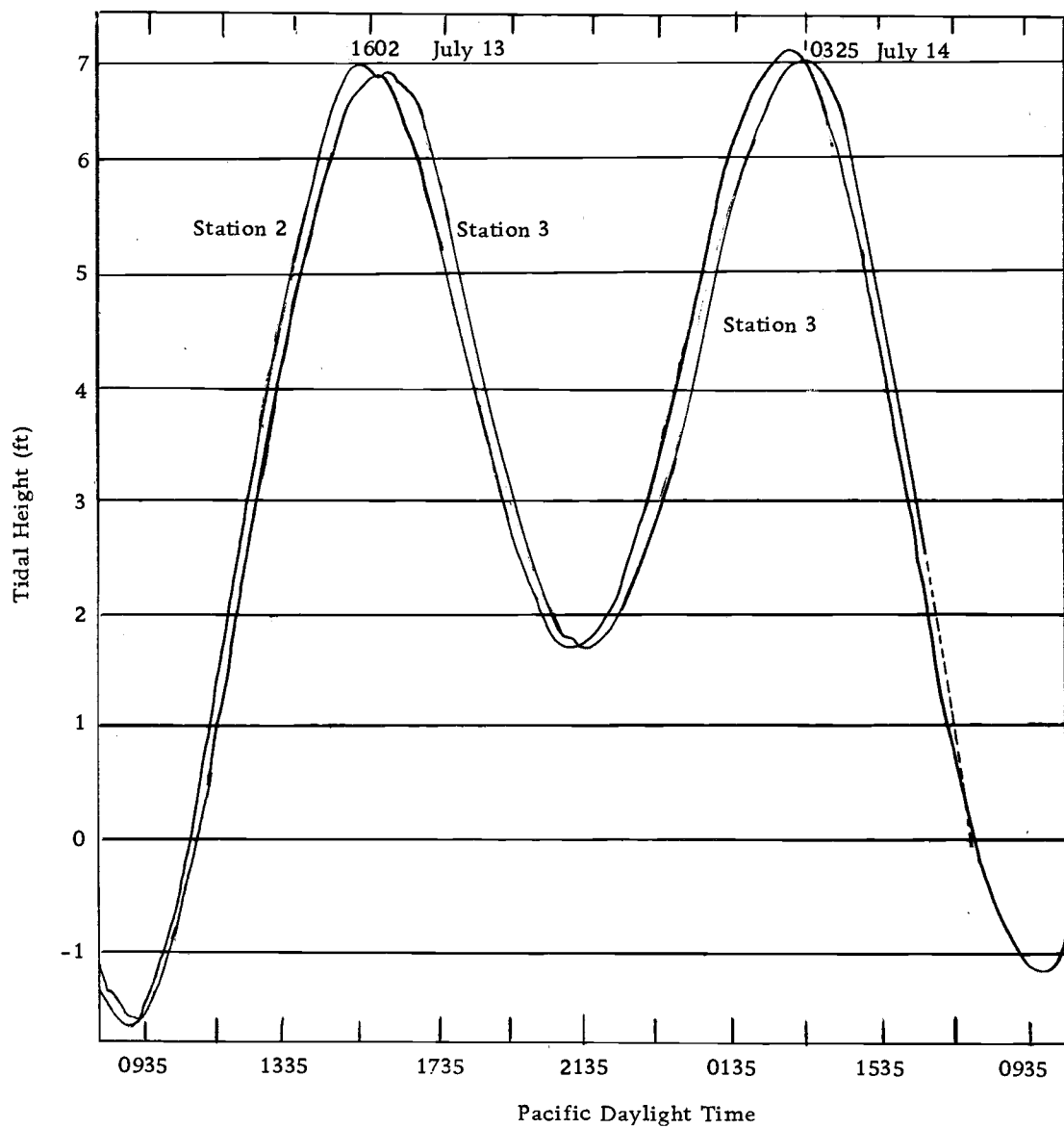
Figure 21. Tidal Relationship Between Stations 2 and 3, Alsea Bay, 1972
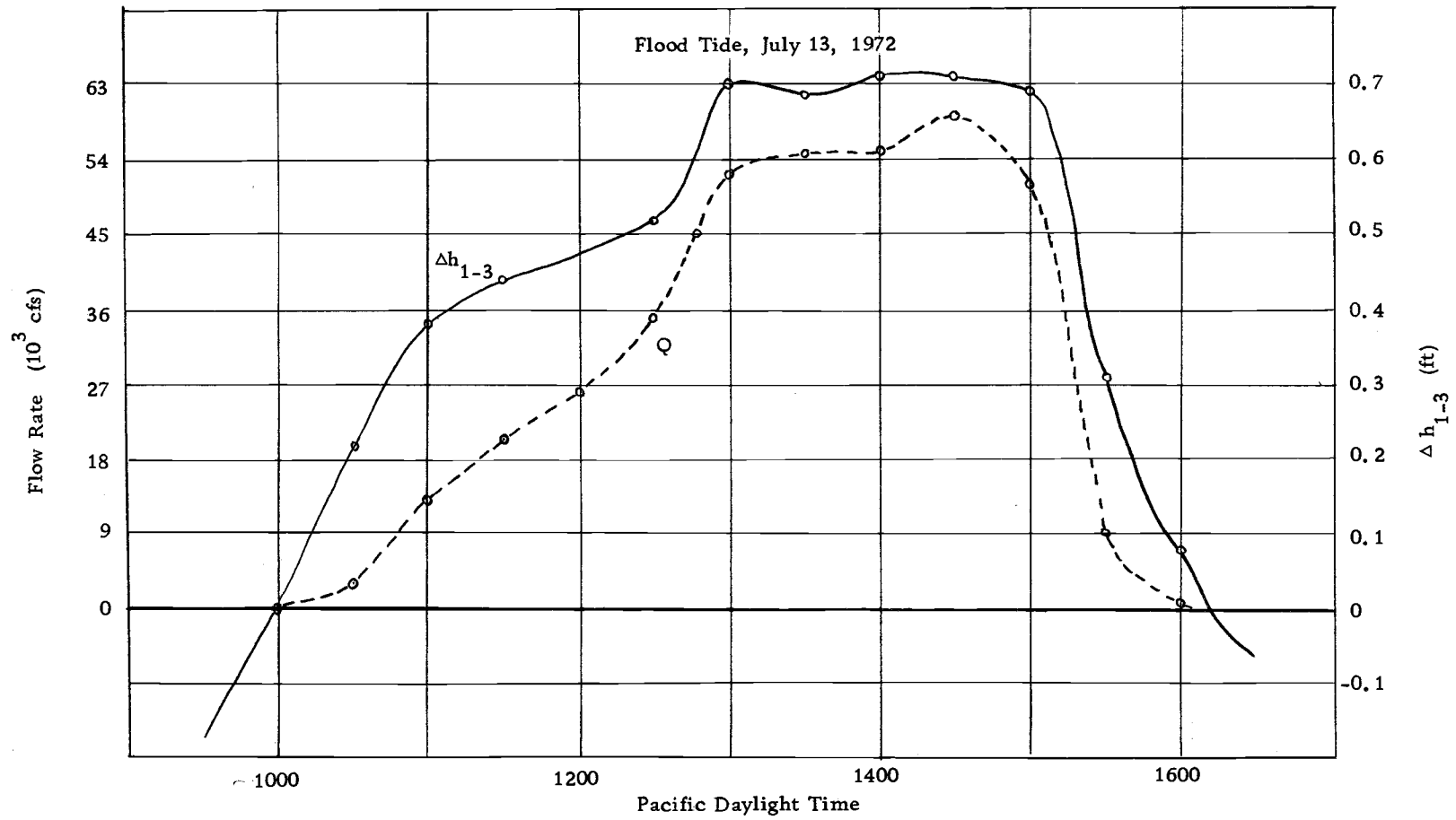
Figure 22. Head Differential and Flow Rate vs. Time, Flood Tide, Alsea Bay, July 13, 1972

sectional area at the narrowest region will be used. From entrance bathymetry measurements this is section d-d of the inlet (see Figure 7 or 14). Even though this is not the minimum cross sectional area at MLLW, for higher tidal stages this section will have the minimum flow area. Taking into account the tidal flats on either side of section d-d, the cross sectional area increases with tidal height as shown in Figures 23 and 24.

Table III summarizes the values from which the Alsea Bay flood tide discharge coefficients were determined.

Ebb Tide Analysis

To establish the relationship between the ocean tidal curve and the tidal curve for the bay side of the entrance for the ebbing tide of July 14th using the criteria mentioned at the beginning of this section, it was necessary to move the entrance tidal curve upward by .14 feet and ahead by 4 minutes, as shown in Figure 25. (This is still well within the limits of error for the tide recording methods used.) Table IV gives the values for the head differential between Stations 1 and 2, Δh_{1-2}, and Q for July 14th, 1972.

Again, calculations to determine C from these values indicate that the tidal response at Station 2 does not seem representative of the tidal response of the bay. From Figure 21, Δh_{2-3} was determined for part of the tidal cycle, since the tide recorder at Station 3
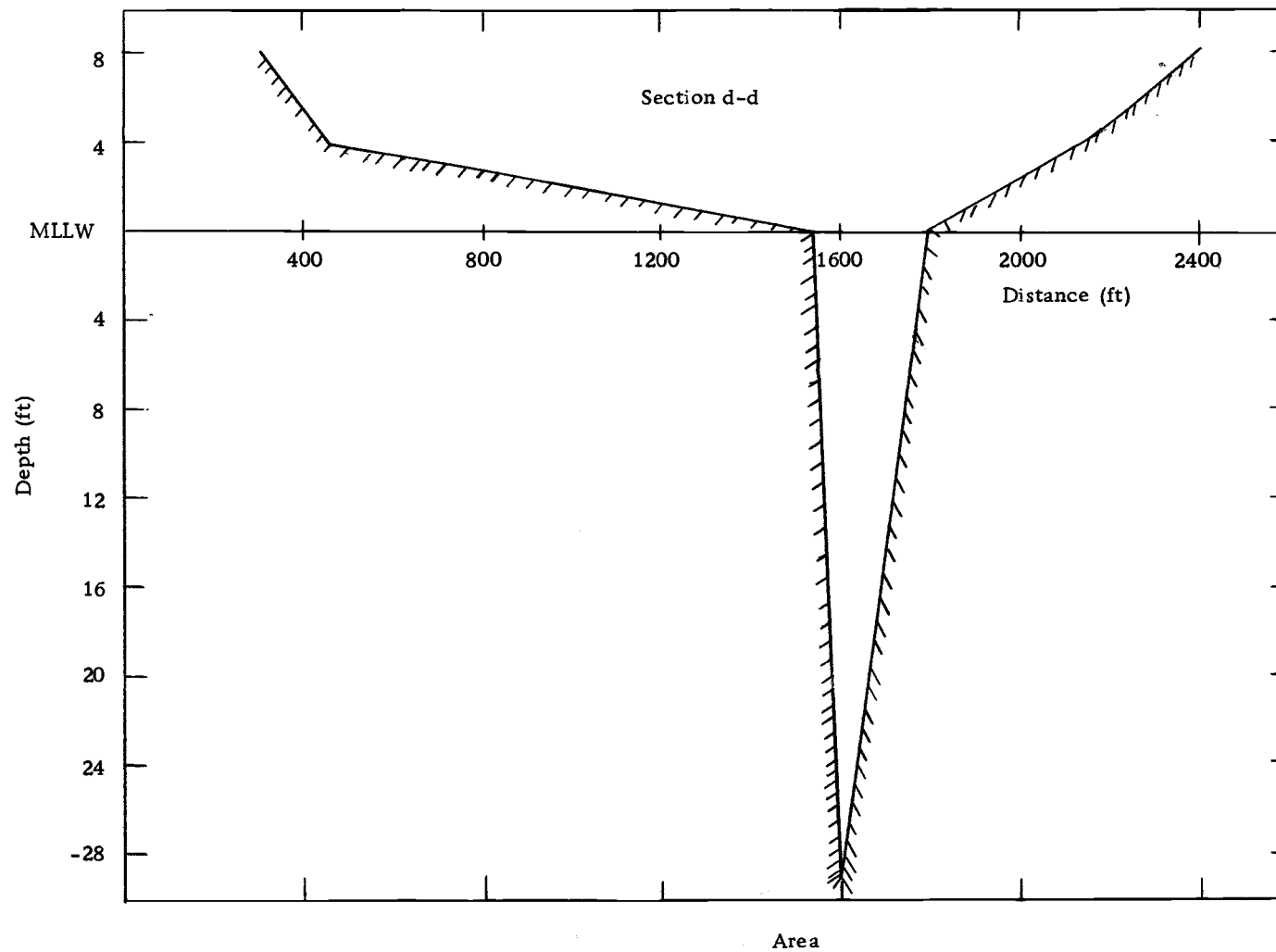
Figure 23. Minimum Area Cross Sectional Profile, Alsea Bay Inlet
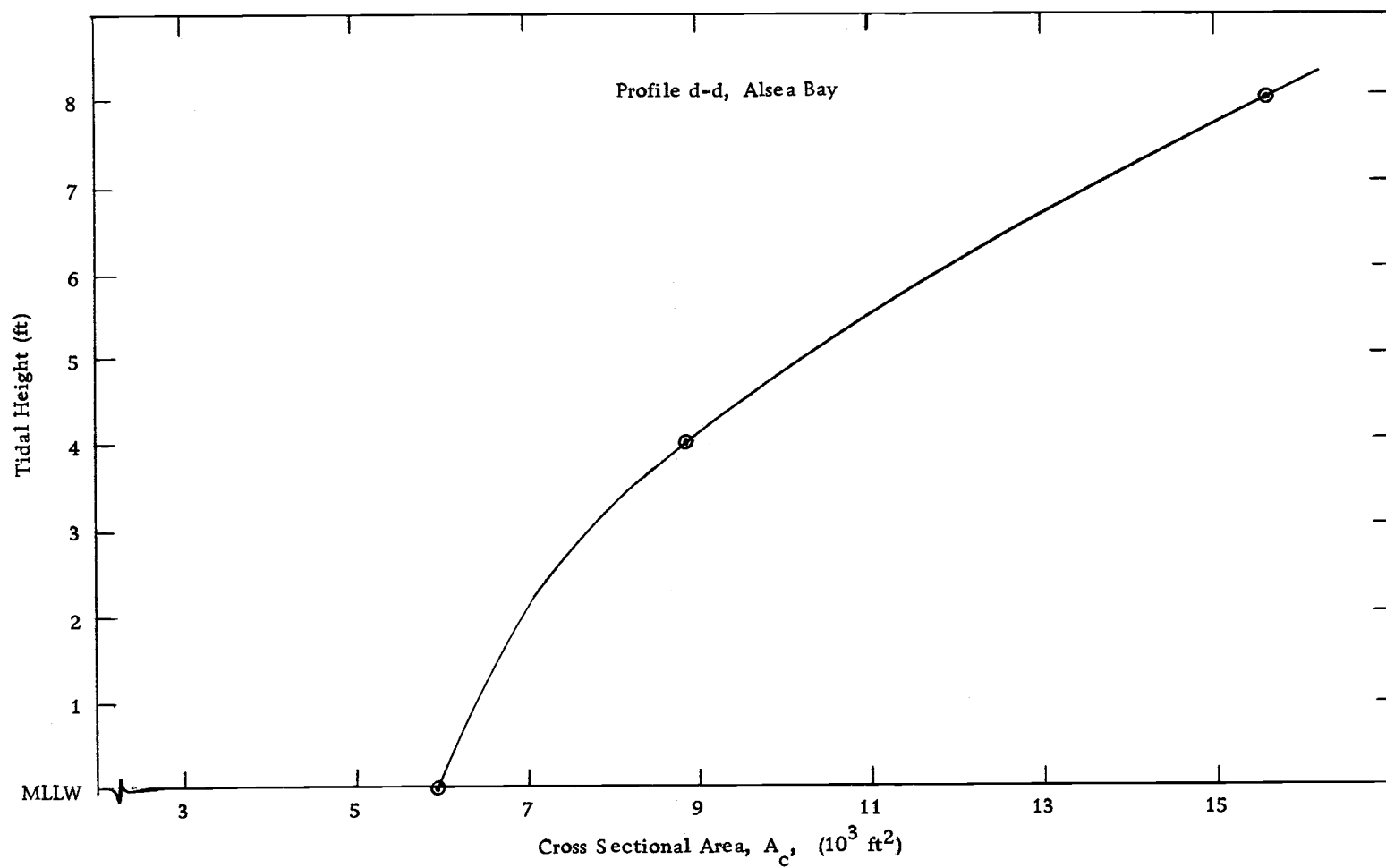
Figure 24. Increase in Cross Sectional Area with Tidal Height, Profile d-d, Alsea Bay

Table III. Discharge Coefficient C, Flood Tide, Alsea Bay

Time (PDT)	Tidal Height (ft)	A_c (ft^2)	Q (10^3 cfs)	Δh (ft)		C
				Δh_{1-2}	Δh_{1-3}	
1030	-0.2	5,900	3.1	.08	.22	.14
1100	0.8	6,380	13.1	.06	.38	.42
1130	1.6	6,700	20.6	.11	.44	.58
1200	2.6	7,400	25.8	14	.47	.63
1230	3.6	8,370	35.0	.16	.52	.72
1300	4.5	9,540	52.1	.25	.70	.81
1330	5.3	10,750	54.6	.26	.68	.77
1400	6.0	11,900	55.0	.31	.71	.68
1430	6.5	12,750	59.8	.32	.71	.70
1500	6.8	13,280	51.2	.31	.69	.58
1530	6.9	13,450	9.1	.19	.31	.15
1600	6.8	13,280	1	.08	.08	.03
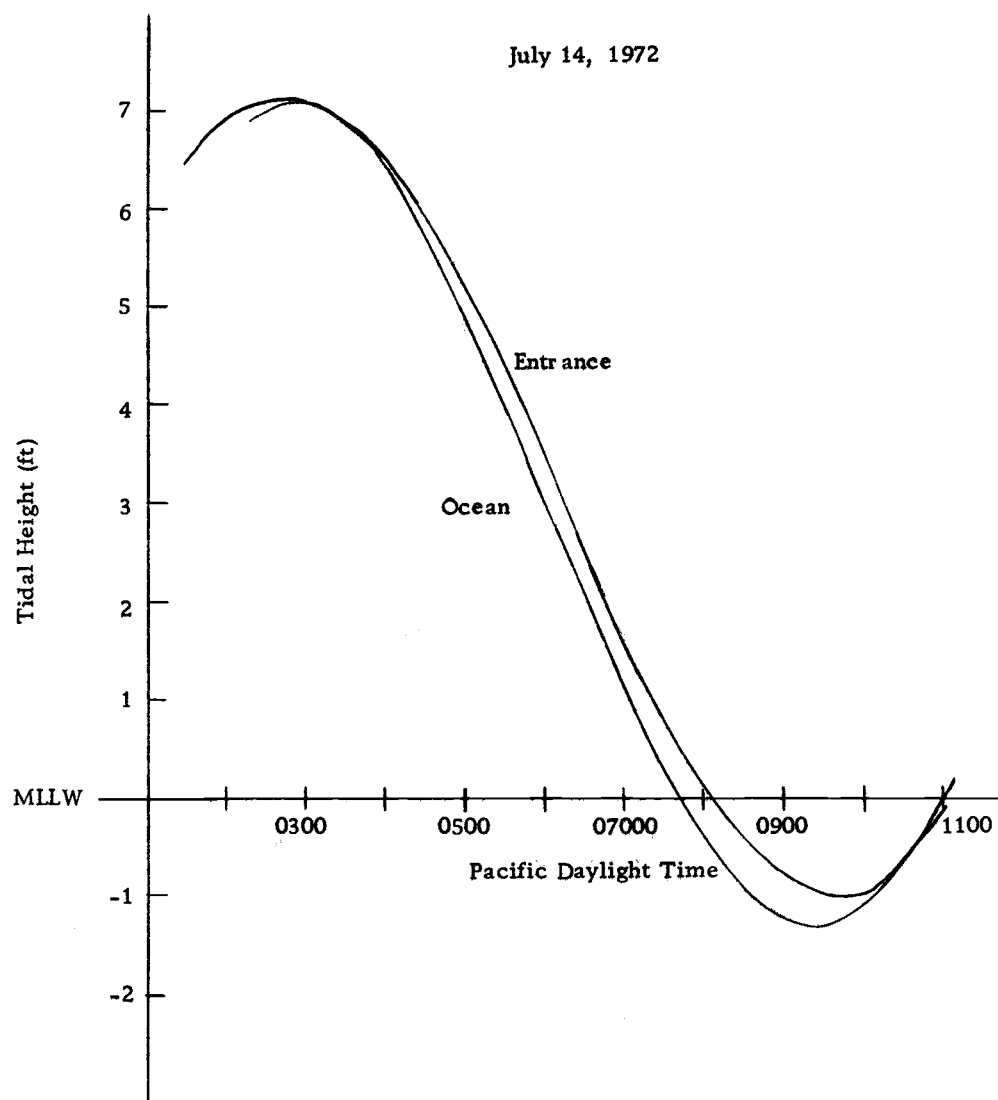
Figure 25. Tidal Relationship Between Stations 1 and 2, Alsea
Bay, July 14, 1972

Table IV. Discharge Coefficient C, Ebb Tide, Alsea Bay

Time	Tidal Height	A_c	Q	Δh (ft)		C
(PDT)	(ft)	(ft^2)	(10^3 cfs)	Δh_{2-1}	Δh_{3-1}^*	
0400	7.5	14,600	22.0	.02	.20	.42
0430	6.9	13,450	32.8	.13	.46	.45
0500	6.2	12,250	42.1	.32	.62	.55
0530	5.3	10,750	46.7	.43	.69	.65
0600	4.3	9,250	47.0	.48	.71	.75
0630	3.3	8,050	44.	.48	63	.87
0700	2.3	7,150	42.3	.45	.55**	.99
0730	1.5	6,650	36.8	.48	.53**	.99
0800	0.8	6,300	28.4	.52	-	.78
0830	0.3	6,050	20.8	.52	-	.60
0900	-0.1	5,900	14.1	.44	-	.45
0930	-0.3	5,900	11.0	.32	-	.41
1000	0	5,940	8.8	.12	-	.54

*corrected for velocity effects past Station 3.
**inferred values

malfunctioned at 0630 hours, July 14th. Using the values that were available up to that time, and inferred values for 0700 and 0730 hours, the values of Δh_{1-3} and Q for July 14th ebb tide are shown in Figure 26. Using these values, the discharge coefficients for this ebb tide were determined, and are also listed in Table IV.

Several items should be examined concerning the values listed in Table IV. The two values of Δh_{2-3} inferred from Figure 22 were obtained by continuing the tidal curve with a straight line. This yields Δh_{1-3} values for 0700 and 0730 which are probably smaller than would have been measured had the tide recorder not malfunctioned. Thus, the discharge coefficient C is probably larger for these times than shown by the calculated values.

A correction for velocity effects has been applied to Δh_{2-3} values for July 14th. Since for an ideal bay one would assume a negligible velocity within the bay, this correction was necessary to account for the high flow rates past Station 3. Manning's equation with an arbitrarily estimated value of n = .02 was used to estimate the water surface slope, with the correction amounting to .02 feet for each foot per second of velocity past Station 3. The maximum correction was .06 feet.
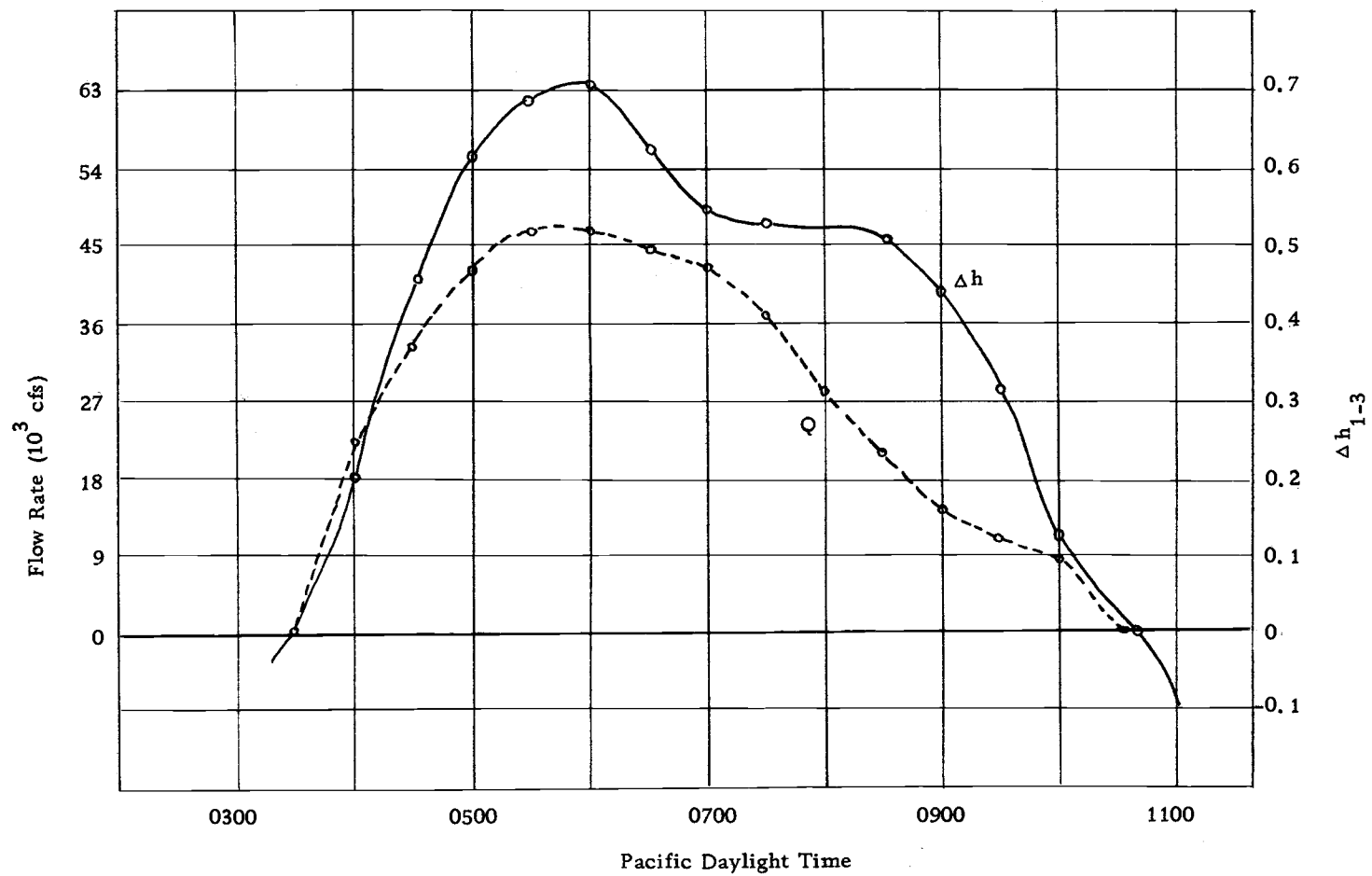
Figure 26. Head Differential and Flow Rate vs. Time, Ebb Tide, Alsea Bay, July 14, 1972

Relationship Between Channel Shape and the Discharge Coefficient

If flow through an estuary entrance can be treated as flow through a nozzle, then one should be able to predict the energy losses across the inlet, based upon a knowledge of the flow rate of water through the entrance and the entrance channel shape.

Energy losses across the inlet can be broken into two main components: friction losses, and entrance-exit losses. Friction losses for the Alsea Bay measurements of July 13 and 14, 1972, will be estimated using the following assumptions:

1. The friction loss will be predicted assuming a uniform velocity along the length of the channel. Since the average cross sectional area along the length of the channel at MLLW is 15% greater than the minimum cross sectional area of the channel at MLLW, this proportion will be assumed to hold also at higher tidal stages. Thus the uniform velocity (hereafter termed V_{ave}) will be computed by dividing the measured flow rate by the average cross sectional area for each time of interest:

$$V_{ave} = \frac{Q}{A_c \, ave} \qquad (11)$$

2. Since the entrance channel is composed mainly of sand with

    some shape irregularity, a value of Manning's n = .025 will be

    assumed, as estimated from Chow (1959).

Using Manning's Equation

$$V = \frac{1.49}{n} \, S^{1/2} \, R^{2/3} \qquad (12)$$

solving for S, and then multiplying by the channel length yields the

head loss due to friction.

$$\text{Friction loss (feet)} = (S) \cdot (L) = \frac{(V_{ave})(n)}{1.49 \; R^{2/3}} \cdot (L), \qquad (13)$$

where n = Manning's friction factor = .025

      R = hydraulic radius (average along length of channel)

      S = water surface slope

and   L = length of entrance channel (feet).

It should be noted that the head loss across the inlet due to fric-

tion is proportional to the square of the velocity. By computing an

average velocity for the entrance channel, the second order effects

have been neglected, thus introducing some error in estimation of

friction losses. However the above method will be useful as a first

approximation in estimating friction losses through the entrance.

Exit losses will be estimated assuming the entrance jet diffuses

into a body of still water. From Bernoulli's equation,

$$\text{exit loss} = K_L \frac{v^2}{2g} \tag{14}$$

where   v = velocity of jet

   g = gravitational acceleration = 32. 3 ft/sec^2

and K_L = exit loss coefficient

Since the narrows of the entrance channel is quite near the bay, for flood tide flows the velocity will be computed by dividing the flow rate by the minimum cross sectional area. This is felt to give the most realistic estimate of exit velocity of the jet into the bay. On ebb flows, however, since gradual channel enlargement occurs seaward of the narrows, the velocity of the jet is calculated using the average cross sectional area. It was felt this would give the most realistic estimate of the velocity of the jet diffusing into the ocean. Entrance losses of water entering the channel are assumed to be negligible for both flood and ebb flows.

Due to the location of tide recorder 2, the measured values of Δh_{1-2} on a flood tide should be a measure of the friction losses across the inlet. This is due to the fact that tide recorder 2 is at the end of the entrance channel, yet the incoming flow has not yet diffused into the bay at that point. This allows us to compare not only the total measured losses with total predicted losses, but also to compare measured friction loss with predicted friction loss and measured exit

losses with predicted exit losses for the flood tide. This comparison

can be made in Table V, where the predicted and measured values of

Δh_{1-3} for the flood tide of July 13, 1972 are shown.

To better illustrate the values given in Table V, Figure 27

shows measured values minus predicted values for friction losses,

exit losses, and total losses across the inlet. At low flow rates

measured losses across the inlet are greater than predicted losses,

while during peak flows the predicted losses are slightly greater than

measured losses. However, considering the accuracy of the tidal

height measurements and the complexity of the inlet, agreement

between predicted values and measured values is quite good. Some

comments should be made concerning the effect of several factors on

losses across the inlet.

1. Mass transport of water across the outer bar due to wave

   action will tend to increase the flow rate over what would be

   expected otherwise. This will tend to increase the predicted

   losses across the inlet. However it is felt this is an insignifi-

   cant factor for most flow rates.

2. Variation in Manning's n has a significant effect on predicted

   friction losses, as shown by the dashed line in Figure 27. A

   value of n = .020 seems to be in better agreement with

   measured friction losses.

Table V. Flood Tide, Predicted Δh and Measured Δh, Alsea Bay

Time (PDT)	Q (10^3cfs)	V_{ave} (fps)	V_{max} (fps)	Predicted Δh (ft)			Measured Δh (ft)		
				friction	exit loss	total	friction	exit loss	total
1030	3.1	.46	.53	0	0	.01	.08	.14	.22
1100	13.1	1.8	2.1	.15	.07	.22	.06	.32	.38
1130	20.6	2.7	3.1	.23	.15	.38	.11	.33	.44
1200	25.8	3.0	3.5	.26	.19	.45	.14	.33	.47
1230	35.0	3.6	4.2	.34	.27	.61	.16	.36	.52
1300	52.1	4.7	5.5	.45	.47	.92	.25	.45	.70
1330	54.6	4.4	5 1	.42	.40	.82	.26	.42	.68
1400	55.0	4.0	4.6	.38	.33	.71	.31	.40	.71
1430	59.8	4 1	4.7	.36	.34	.70	.32	.39	.71
1500	51.2	3.3	3.8	.23	.22	.45	.31	.38	.69
1530	9.1	0.6	0.7	.01	.01	.02	.19	.12	.31
1	2	3	4	5	6	7	8	9	10
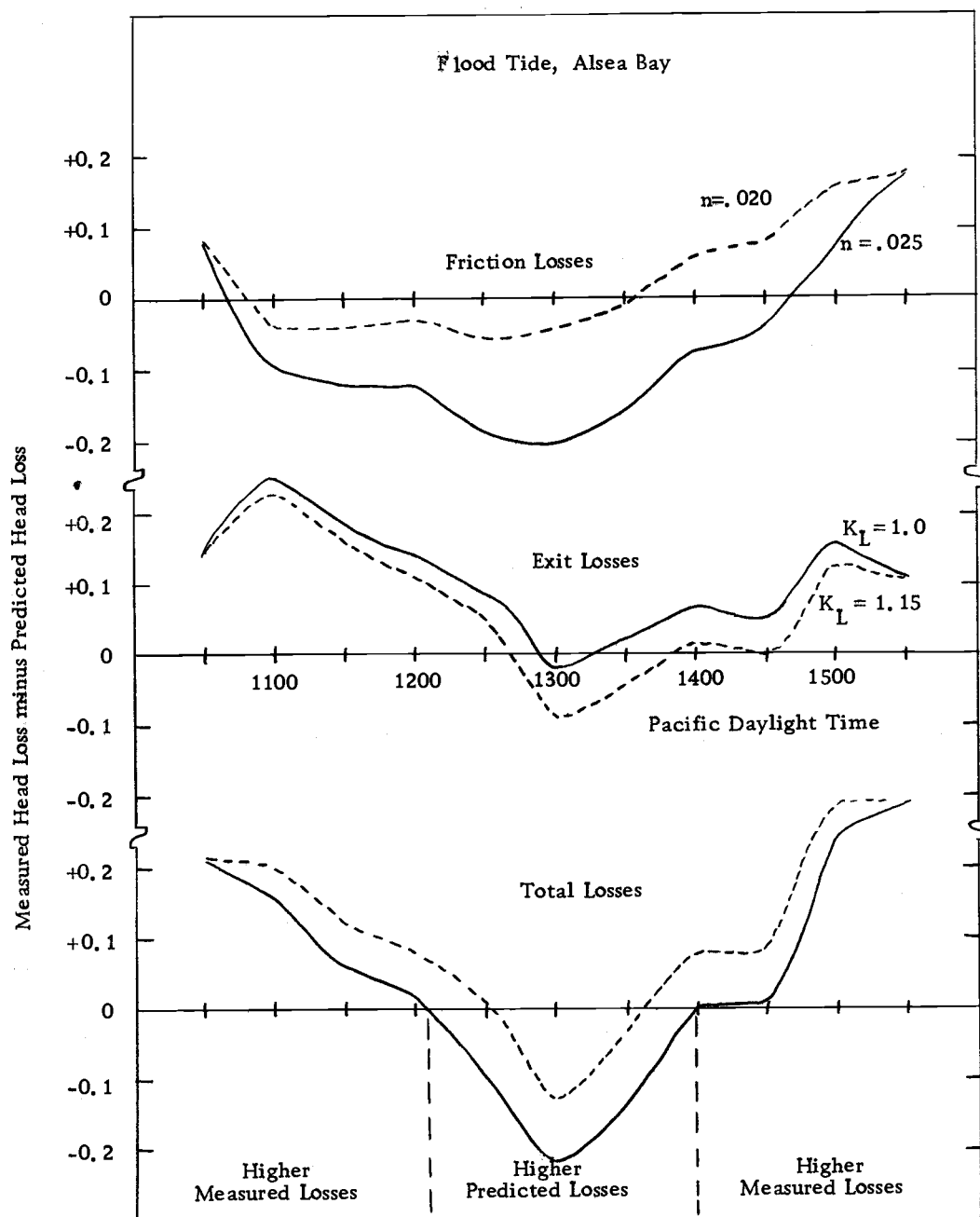
Figure 27. Measured Inlet Losses minus Predicted Inlet Losses, Ebb Tide, Alsea Bay

3. In predicting friction losses across the inlet, an average value of the hydraulic radius for the entrance <u>channel</u> was used. As tidal stage is increased and the tidal flats on either side of the inlet become covered, the hydraulic radius will decrease, increasing the frictional effects on flows. In estimating the frictional effects illustrated in Figure 27, the hydraulic radius for the channel was used. Therefore the predicted frictional effects at higher tidal stages are smaller than expected.

4. Due to a non-uniform velocity distribution in the inlet, the value of the loss coefficient K_L in determining exit losses would be expected to be greater than 1.0. From Vennard (1940, p. 311), a loss coefficient of 1.15 would be a more suitable value, and is also illustrated in Figure 27.

For the ebb tide of July 14, 1972, friction losses and exit losses were predicted similarly to the flood tide of July 13th, however due to the placement of the tide recorders it is not possible to separately measure the friction and exit loss terms. Therefore, comparison can only be made between total predicted losses and total measured losses across the inlet. These values are given in Table VI, and are illus-trated in Figure 28. Agreement between predicted and measured losses across the inlet is not nearly as good as for the flood tide. During periods of high flow rates the predicted losses are nearly double measured losses, while at low ebb flows and low tidal stage the

Table VI.   Ebb Tide, Predicted Δh and Measured Δh, Alsea Bay

Time PDT	Q (10^3 cfs)	V_{ave} (fps)	Predicted Δh_{3-1}			Measured Δh_{3-1}
			friction	exit loss	total	
0400	22	1.3	.03	.03	.06	.20
0430	32.8	2.1	.09	.07	.16	.46
0500	42.1	3.0	.20	.14	.34	.62
0530	46.7	3.8	.34	.22	.56	.69
0600	47.0	4.4	.48	.30	.78	.71
0630	44.4	4.8	.61	.36	.97	.63
0700	42.3	5.1	.67	.40	1.07	.55
0730	36.8	4.8	.71	.36	1.07	.53
0800	28.4	3.9	.52	.24	.76	.52
0830	20.8	3.0	.31	.14	.45	.52
0900	14.1	2.1	.16	.07	.23	.44
0930	11.0	1.6	.09	.04	.13	.32
1000	8.8	1.3	.06	.03	.09	.12
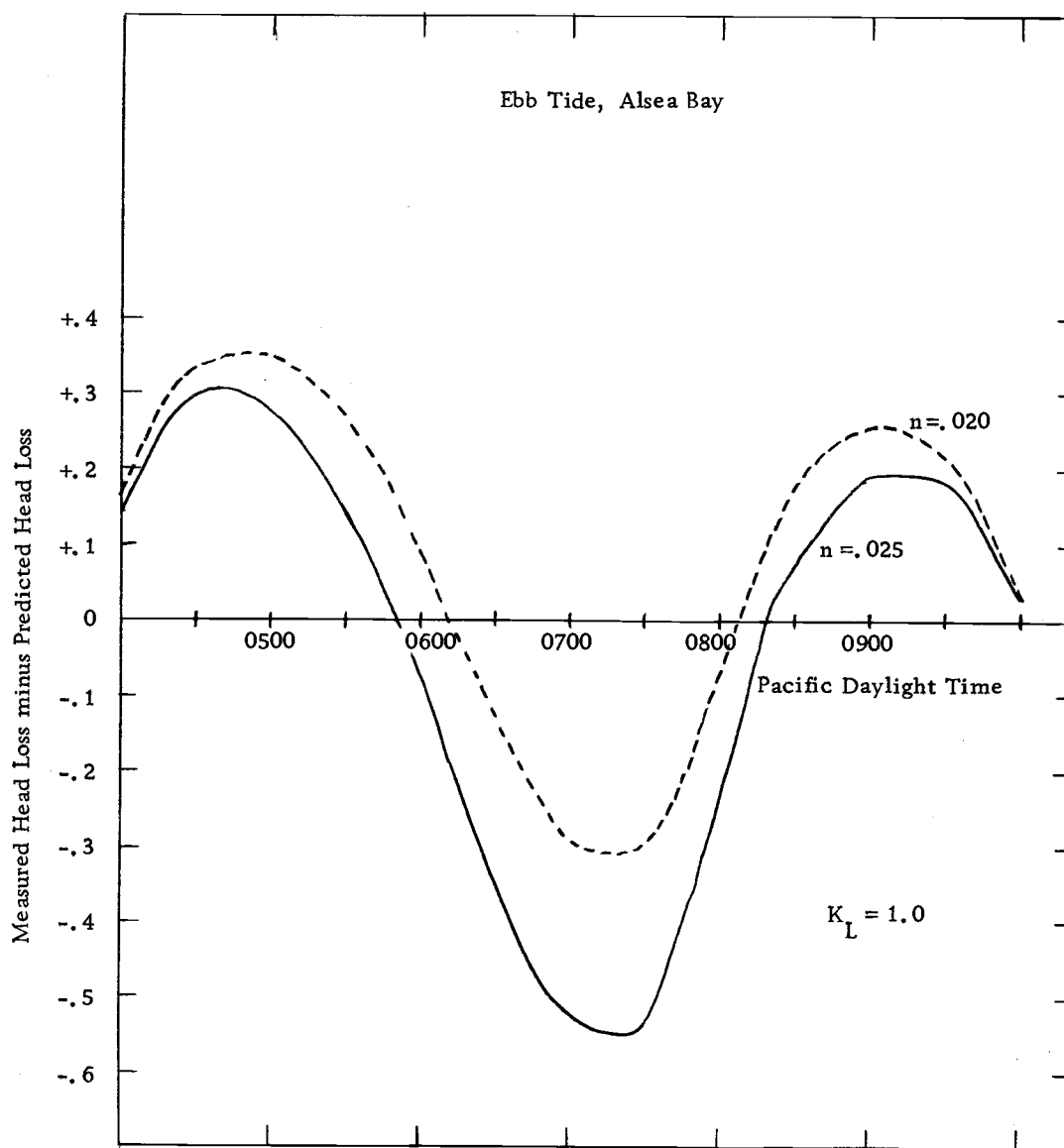
Figure 28. Measured Inlet Losses minus Predicted Inlet Losses, Ebb Tide, Alsea Bay

measured losses are greater than what would be expected. This

latter condition may be due to a constriction of the ebb flows caused

by the outer bar. However, at high flow rates the discrepancy between

measured and predicted values is presently unexplainable. An

apparent cyclic variation in Figure 28 suggests the discrepancy

between measured and predicted values is due to physical phenomena

rather than caused by random errors in data collection.

Relationship of the Discharge Coefficient to Velocity Through the Inlet

In order to better understand the variation in the discharge

coefficient over a tidal cycle, the relationship of the discharge

coefficient to velocity through the inlet was examined. As shown in

Figure 29, the discharge coefficient was found to be proportional to

the velocity through the inlet raised to the 0.8 power, or

$$C \, \alpha \, V^{0.8} .$$

Velocity through the inlet was determined by dividing the flow rate by

the cross sectional area of section d-d.

The relationship of the discharge coefficient to several other

parameters was also explored. The discharge coefficient was found

to have a strong relationship to the Froude number, as might be

expected. One might also expect the discharge coefficient to have a

strong dependency on the Reynolds number, $\dfrac{VH}{\nu}$. However, correlation
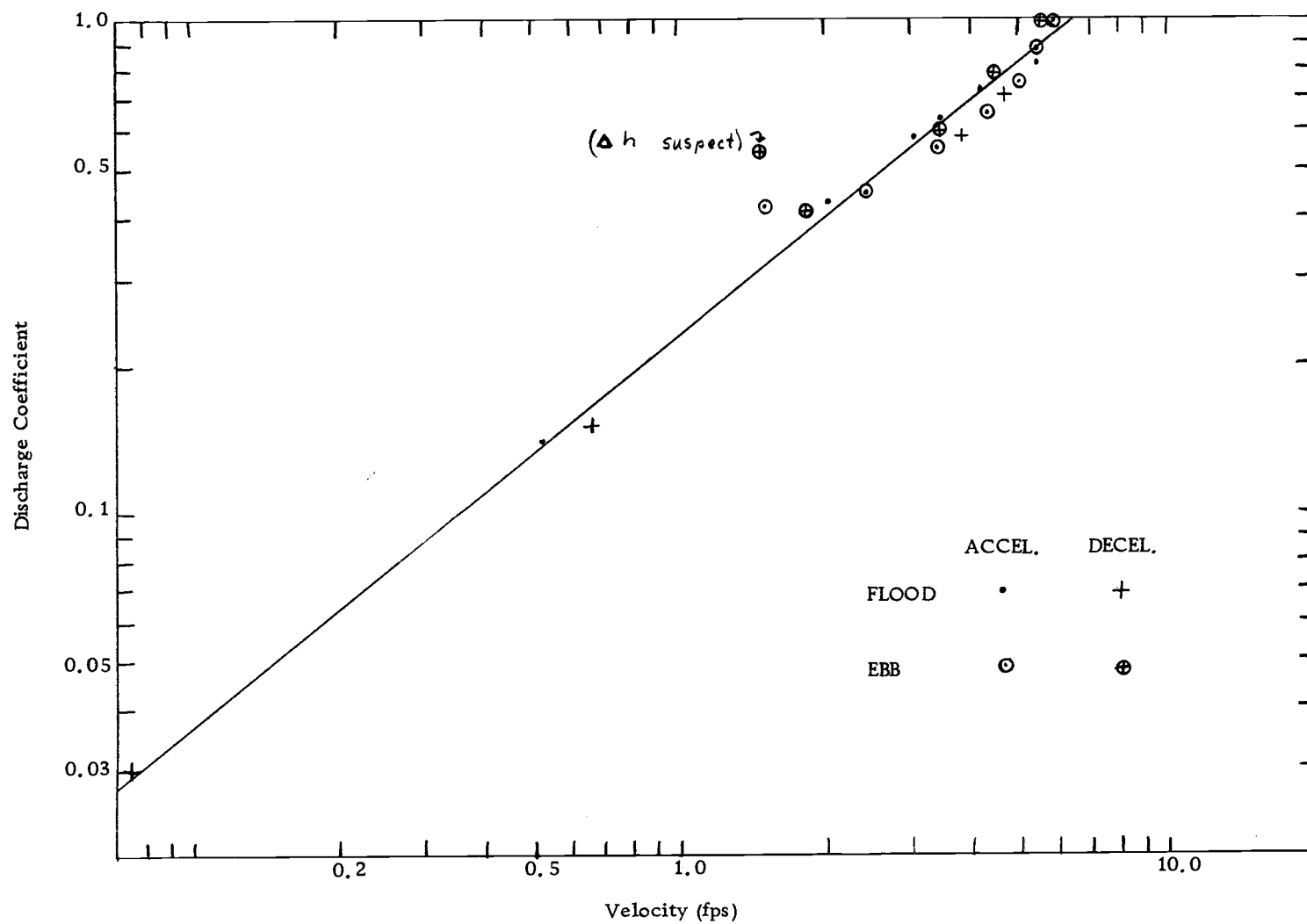
Figure 29.   Relationship of Discharge Coefficient to Velocity

between the discharge coefficient and the Reynold's number of flow

through the inlet was found to be insignificant.

IX. CONCLUSIONS

Energy losses for tidal flows through a natural estuarine inlet were measured and compared with values predicted from measurements of the inlet bathymetry. Both flood and ebb tidal flows were studied. Favorable comparison of predicted and measured losses across the inlet for a flooding tide indicate that the inlet shape and hydraulic characteristics can be critical factors affecting the tidal response of the estuary during the flooding tide. Energy losses for incoming flows were shown to be predictable based upon a knowledge of the inlet bathymetry and the tidal fluctuations of the bay and ocean.

Comparison of predicted and measured losses across the inlet for an ebbing tide shows that the inlet shape is not the predominant factor controlling ebb flows, at least for the single estuary studied. Resistance to flow occurring upstream in the estuary may determine the rate at which the estuary empties.

Energy losses for both flood and ebb flows were estimated by separating losses due to friction and losses due to expansion of the fluid jet. Friction and expansion losses can be combined into a single discharge coefficient C, which is related to the flow through the inlet by an expression often used for flow through orifices,

$$Q = C A_{c(inlet)} \sqrt{2g \, \Delta h} \, . \tag{7}$$

For a nozzle or orifice the discharge coefficient C is usually a

constant for fully developed turbulent flow. For an estuarine inlet, C is not a constant over the tidal cycle, but varies as a function of flow rate and tidal stage. For the flood tide examined the value of C varied from .03 to .81, while for the ebb tide C varied from .41 to .99. There was found to be a strong relationship between the discharge coefficient and velocity through the inlet. There did not appear to be a conclusive relationship between the dischrage coefficient C and the Reynolds number of flow through the inlet.

In applying the results of this experiment to a general understanding of estuarine hydraulics, it should be considered that the estuary studied, Alsea Bay, is a very complex combination of channels, broad tidal flats, and embayments. The inlet is subject to strong wave action and high rates of littoral transport of sand. It is not a simple bay-ocean system as depicted in the theoretical considerations of Chapter II of this report. Yet, particularly for a flooding tide, good results were obtained by assuming the estuary to be a simple bay-ocean system, and flow through the inlet to be affected mainly by friction and entrance-exit loss terms. This indicates that the prediction of energy losses across an inlet based upon the geometry of the entrance region can be a valuable means of understanding the tidal response of an estuary and determining the effects of changes in the inlet region on the tidal response of the estuary or lagoon.

BIBLIOGRAPHY

Brown, Earl I. 1928. Inlets on Sandy Coasts. Proceedings of the American Society ofCivil Engineers. Volume 54, pp. 505-553.

Bruun, P. 1966. Tidal Inlets and Littoral Drift, Stability of Coastal Inlets. Volume 2, Technical University of Norway, 123 pages.

Bruun, P. and F. Gerritsen. 1961. Stability of Coastal Inlets, North Holland Publishing Company, Amsterdam, 123 pages.

Chow, Ven Te. 1959. Open Channel Hydraulics, McGraw-Hill Book Company, Incorporated. 660 pages.

Glenne, B., C. Goodwin and C. Glanzman. 1971. Tidal Choking. Journal of Hydraulic Research, Volume 9, No. 3, pp. 321-332.

Goodwin, C. R. and B. Glenne. 1970. Tidal Study of Three Oregon Estuaries. Bulletin No. 45, Engineering Experimental Station, Oregon State University, Corvallis, Oregon, 33 pages.

Ippen, A. T. 1966. Estuary and Coastline Hydrodynamics. McGraw-Hill Book Company, New York, 744 pages.

Keulegan, G. H. 1967. Tidal Flow in Entrances, Water Level Fluctuations of Basins in Communication With Seas. Technical Bulletin No. 14, Corps of Engineers, U. S. Army, 89 pages.

Marriage, L. D. 1958. The Bay Clams of Oregon, Oregon State Fish Commission Educational Bulletin No. 2, Portland, Oregon, 29 pages.

O'Brien, M. P. 1969. Equilibrium Flow Areas of Inlets on Sandy Coasts, Proceedings of the American Society of Civil Engineers, Hydraulics Division, Volume 95. February 1969.

O'Brien, M. P. 1971. Notes on Tidal Inlets on Sandy Shores, Hydraulic Engineering Laboratory, University of California, Berkeley, 52 pages.

Oliveira, J. B. Mota. 1971. Natural Flushing Ability in Tidal Inlets, National Laboratory of Divil Engineering, Lisbon, Portugal, 19 pages.

Sager, R. and E. McNair, Jr. 1973. Galveston Bay Hurricane Surge Study. Technical Report H-69-12, Corps of Engineers, U. S. Army, 2 Reports, 100 pages.

Vennard, John K. 1940. Elementary Fluid Mechanics, 4th Edition, John Wiley and Sons, Inc. , 570 pages.

APPENDIX A

ALSEA BAY TIDAL DATA

In support of general circulation studies of Alsea Bay, tidal

records were obtained at nine stations.   Three of these, Stations 1,

2, and 3, have been previously described in this report.   Following

is a brief written description of the remaining six stations.   The

location of these stations was shown in Figure 4.

Station 4.   Located on the highway 101 bridge abutment in

the center of the main channel.

Station 5.   Located in the marina boat basin at the mouth of

Lint Slough.

Station 6.   Located on a piling of the old railroad trestle at

Bayview.   This station is dry at low tide.

Station 7.   Located on a private dock at the end of Moffitt

Road.   This station is dry at extremely low tides.

Station 8.   Located on an old piling 1/4 mile downstream from

the entrance to Drift Creek.

Tidal data gathering at these stations was somewhat sporadic,

beginning at Stations 5 and 9, then progressing to different areas of

the bay depending upon specific studies and the ability to maintain

and service the tide recording stations.   This tidal data for Alsea

Bay is contained in Table AI.

If the mean time lag of the tidal wave moving up the bay is

Table AI. Tidal Data, Alsea Bay, 1972

					Station 5						
Date	Time (PDT)	Height (ft above MLLW)	Date	Time	Height	Date	Time	Height	Date	Time	Height
June 22	11:50	4.85	June 28	01:35	7.95	July 4	01:03	1.30	July 15	04:20	6.43
	16:20	3.03		09:40	-0.45		06:35?	5.15		10:37	0.08
	22:13	7.08		15:37	6.25		12:50	1.45		--	--
June 23	06:05	-0.10		--	--		19:03	7.75		22:28	--
			June 29	02:21	7.49	July 5	02:29	0.65	July 16	05:30	--
				10:02	-0.54					11:29	--
				16:10	6.21					17:44	--
June 24	17:50	3.43		21:23	2.72					24:13	--
	23:18	7.55	June 30	02:52	7.21	July 11	14:50	6.59	July 17	05:48	--
June 25	07:22	-0.52		10:28	-0.43		20:12	2.32		11:35	--
	13:48	5.65		16:37	6.33	July 12	01:32	8:32			
	18:32	--		22:29	2.33		09:38	-0.59			
	23:58	--	July 1	03:58	6.60		--	--			
June 26	--	--		10:58	-0.24		20:51	2.21			
	08:02	--		17:09	6.71	July 13	02:28	8.06			
	14:30	0.35		23:08	2.11		10:07	-0.49			
	19:25	3.19	July 2	04:45	6.41		16:09	7.07			
June 27	00:50	7.76		--	--		21:58	2.02			
	08:59	-0.54		18:00	7.31	July 14	03:19	7.28			
	15:10	5.95	July 3	00:20	1.96		10:24	-0.28			
	20:00	3.10		05:53	5.93		16:37	7.03			
				--	--		22:37	1.83			
				18:23	7.45						

Table AI. (Continued)

		Station 4						Station 6		
Date	Time	Range	Date	Time	Range	Date	Time	Height (ft above MLLW)	Date	Time
July 12	L 20:40		July 16	H 04:55		June 29	16:04	6.09	July 14	H 03:23
		5.87			5.0	June 30	02:49	7.16		L 10:46
July 13	H 02:15			L --		July 2	04:53	6.18		H 16:42
		9.28			--	July 3	05:55	5.73		L --
	L 09:20			H 17:33			--	--	July 16	H 05:10
		--			5.3		18:26	7.31		L 11:38
	H			L 24:02			--	--		
		5.10			3.72	July 4	06:50	5.12		
	L 21:38			H 05:40			--	--		
July 14	H 03:14				3.7		18:56	8.38		
		8.03		L 11:30		July 7	11:28	5.28		
	L 10:09						22:51	7.71		
		--				July 11	H 14:51			
	H 16:29						L 20:34			
		5.42				July 12	H 01:36			
	L --						L --			
		--					H 15:10			
July 15	H --						L 21:01			
		6.30				July 13	H 02:28			
	L --						L --			
		--					H 16:02			
	H 17:10						L 22:02			
		5.3								
	L 23:10									
		4.25								

Table AI. (Continued)

Station 7

Date	Time (PDT)	Range (ft)
June 26	L 19:29	
		4.62
June 27	H 00:50	
June 29	H 02:21	
	--	
	--	
	L 21:32	
		4.06
June 30	H 03:02	
		--
	L --	
		--
	H 16:50	
		--
	L 22:30	
		4.33
July 1	H 03:55	
		6.5
	L 11:19	
		--
	H --	
		--
	L 23:25	
		4.26

Date	Time (PDT)	Range (ft)
July 2	H 04:55	
		5.73
	L 11:40	
		6.75
	H 18:15	
		--
	L --	
		--
July 3	H 00:30	
		3.96
	L 06:00	
		4.77
	H 12:15	
		--
	L --	
		6.04

Date	Time (PDT)	Range (ft)
July 4	H 01:40	
		3.77
	L 06:03	
		--
	H 12:40	
		6.2
	L 19:20	
		6.4
July 5	H 01:55	
		4.08
	L 07:32	
		--
	H 19:24	
July 11	H 15:00	
		4.32
	L 20:20	

Table AI. (Continued)

Date		Time (PDT)	Date		Time	Date		Time
June 22	H	22:12	July 1	L	23:43	July 4	L	01:50
							H	07:00
June 27	L	20:20	July 2	H	05:03		L	--
	H	01:48		L	--		H	19:24
				H	--			
June 29	H	02:30		L	23:53	July 11	H	15:05
	L	--					L	20:35
	H	16:25	July 3	H	06:11			
	L	21:55		L	--	July 12	H	01:40
				H	18:30			
June 30	H	03:15						

Table AI. (Continued)

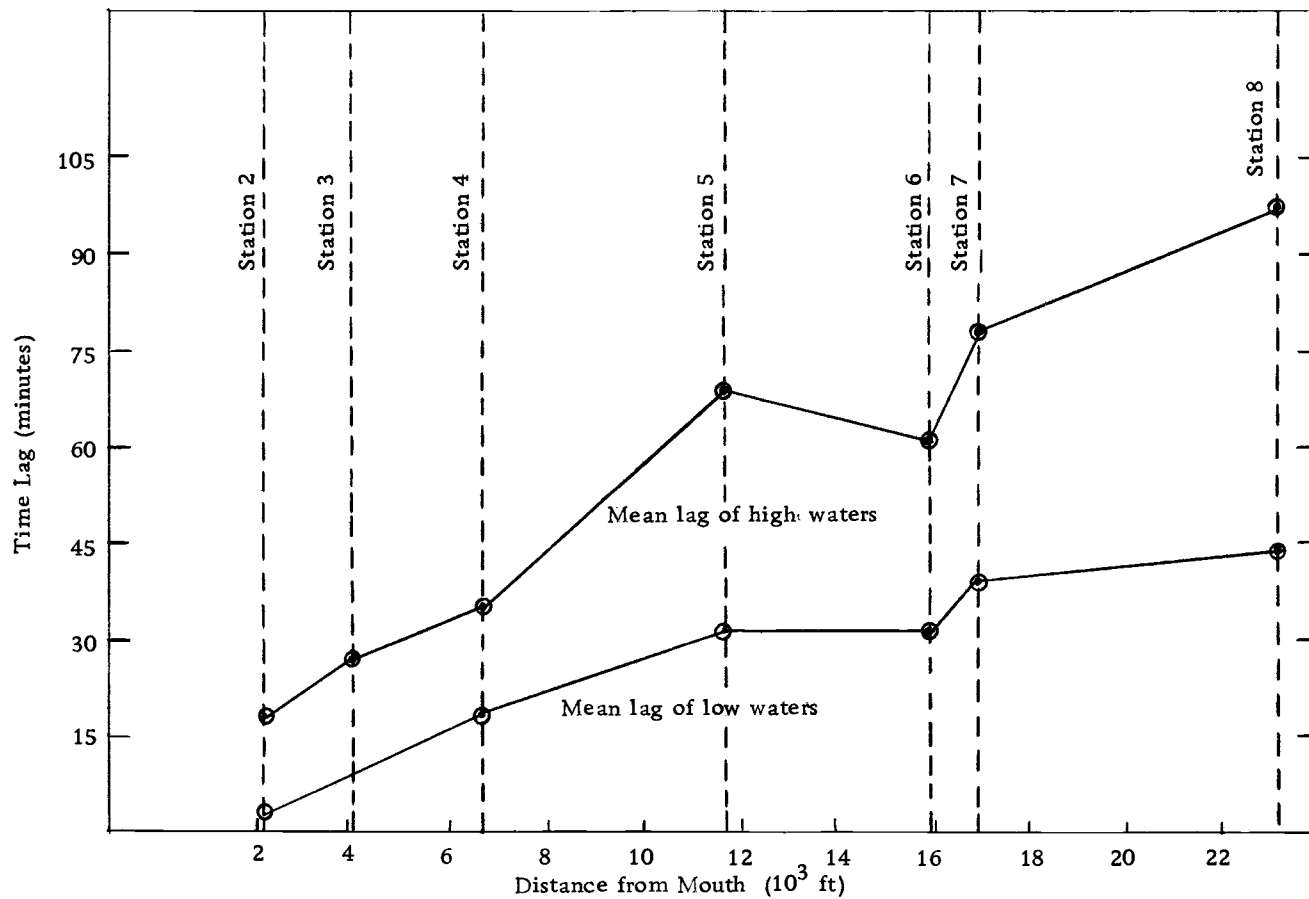|				Station 9				
Date	Time	Height (ft) (above MLLW)	Date	Time	Height	Date	Time	Height
June 20	14:17	2.56	June 27	20:05	2.82	July 3	00:22	1.85
	20:57	7.34					05:55	5.88
			June 28	01:38	7.69		--	--
June 21	--	--		--	--		18:30	7.46
	11:42	5.20		15:40	6.00			
	--	--		20:38	2.74	July 4	--	--
	21:42	6.66					07:05	5.17
			June 29	02:20	7.52		12:52	1.61
June 22	--	--		--	--		19:10	7.74
	--	--		16:12	6.24			
	16:57	2.95		21:29	2.62	July 7	15:55	2.91
	22:15	6.98					22:04	8.46
			June 30	02:59	7.22			
June 23	--	--		--	--	July 8	--	--
	12:35	4.87		17:19	6.53		12:30	5.99
				23:14	1.90			
June 24	17:55	3.3						
	23:25	7.52	July 2	04:47	6.24			
June 25	--	--						
	13:55	5.28						
	18:38	--						
	--	--						

Figure A1.   Mean Time Lag of High and Low Waters, Alsea Bay, 1972

plotted against the distance from the entrance (Figure Al), an

interesting phenomenon can be observed. High tide occurs at nearly

the same time at Station 5 and Station 6, indicating the north and

south parts of the bay fill at about the same rate. However low tide

occurs earlier at Station 6 than Station 5, indicating the northern

section of the bay empties before the southern section. This is in

spite of the fact that the old north channel has been blocked, and the

south channel has been dredged to increase flow in this channel. The

north channel of the bay is presently filling in with fine silts and muds,

though hydrographic investigations indicate the mean depth at MLLW

is still greater than that of the south channel.

Since very few offshore tidal measurements have been made

along this section of the Pacific Coast, the damping of the tidal

ranges inside the bay relative to ocean tidal ranges was examined.

The relative range (ratio of ocean tidal range to bay tidal range)

was plotted against the ocean range, as shown in Figure A2. This

relative range ratio, commonly called the tidal choking coefficient,

was found to be fairly independent of the absolute ocean tidal range.

A choking coefficient of about .82 was found to occur between the

ocean and Station 2, just within the inlet. Choking continued between

Stations 2 and 5, with a choking coefficient of about .78 at Station 5.

Figure A2.   Tidal Choking for Alsea Bay Inlet, 1972

82

APPENDIX B

ADDITIONAL REFERENCES CONCERNING ALSEA BAY

Selected bibliography of other literature concerning Alsea Bay and vicinity. From a report in prepartion for the Oregon Coastal Conservation and Development Commission, compiled March 1973.

Burt, W. V., and McAllister, B., "Hydrography of Oregon Estuaries, June 1956 to September 1958," Office of Naval Research Reference 58-6, School of Science, Oregon State College, Corvallis, Ore., 1958.
    18 pp. Gives temperature and salinity data in tabulated form for Alsea, Columbia, Coos, Nehalem, Netarts, Siletz, Siuslaw, Tillamook, Umpqua, and Yaquina estuaries between June 1956 and September 1958.

Goodwin, C. R., Emmet, E. W., and Glenne, B., "Tidal Study of Three Oregon Estuaries," Bulletin No. 45, Engineering Experiment Station, OSU, Corvallis, Ore., May, 1970.
    33 pp. Discusses tidal elevations and tidal currents in Yaquina, Alsea, and Siletz estuaries.

Helland, R. O., "Water Power of the Coast Streams of Oregon," U. S. Dept. of the Interior, Feb., 1953.
    46 pp. Gives a general description of Oregon coastal streams and discusses them in terms of water supply and storage sites and plan of development, with conclusions regarding potential for power. Includes the Nehalem Rivers, Wilson and Trask Rivers (Tillamook Bay), Nestucca River, Siletz River, Alsea River, Siuslaw River, Coos River, and Coquille River.

Johnson, J. W., "Tidal Inlets on the California, Oregon, and Washington Coasts," Hydraulic Engineering Laboratory HEL 24-12, Univ. of Calif,, Berkeley, Calif., Feb., 1972.
    156 pp. Discusses factors affecting the stability of tidal inlets and gives characteristics of California, Oregon, and Washington coastal inlets including number of jetties, tidal data, bay dimensions, and wave climate.

Marriage, L. D., "The Bay Clams of Oregon," Fish Commission of Oregon, Educational Bulletin #2, Portland, Ore., 1958.
    22 pp. Describes the various types of clams generally found in Oregon estuaries and also lists the types present in each specific estuary. Also gives estuary surface areas.

Matson, A. L., "Zooplankton and Hydrography of Alsea Bay, Oregon, September 1966 to September 1968," thesis presented to Oregon State University at Corvallis, Ore., in June, 1972, in partial fulfillment of the requirements for the degree of Doctor of Philosophy.

Oregon State Water Resources Board, "Mid-Coast Basin," Salem, Ore., May, 1965.
    121 pp. Describes the Mid-Coast Basin, including the Salmon, Siletz, Yaquina, Alsea, Yachats, and Siuslaw Rivers and their drainage basins, as follows: physical features, economic factors, surface water and ground water, water use and associated problems, water control and developmental potential. Includes maps.
    Work on an updated version is underway and scheduled for publication in 1974.